

Fabrication and Characterization of Layer by Layer Assembled Single and Dual- Electrochrome Electrochromic Devices

Reza Montazami

Thesis submitted to the faculty of the Virginia Polytechnic Institute and State University
in partial fulfillment of the requirements for the degree of

Master of Science
In
Materials Science and Engineering

James R. Heflin
Donald Leo
Abby W. Morgan

(December 4, 2009)
Blacksburg Virginia

Keywords: Layer-by-layer, Electrochromism, Ionic Self Assembled Multilayers, ISAM

Fabrication and Characterization of Layer by Layer Assembled Single and Dual-Electrochromic Electrochromic Devices

Reza Montazami

ABSTRACT

This thesis presents applications of the layer-by-layer (LbL) assembly technique in fabrication of thin films with a primary focus on design and development of electrochromic devices. The optical properties of electrochromic materials change as they alter between redox states. The morphology and properties of LbL-assembled thin films can be modified by varying several processing factors such as dipping duration, ion type, ion concentration, pH, molecular weight, and ionic strength. In the present work, several factors of LbL assembly process were manipulated to tailor electrochromic thin films of desired attributes.

An electrochromic device (ECD) with fast optical switching speed was designed and constructed based on poly(3,4-ethylenedioxythiophene):poly(styrenesulfonate) (PEDOT:PSS). This device exhibited optical switching speeds of 31 and 6 ms for coloration and decoloration respectively, on a 60 mm² area.

Poly(aniline 2-sulfonic acid) (PASA) is a relatively new ionic polymer, and its electrochromic properties have not been previously investigated in much detail. PASA thin film showed several redox states corresponding to color changes from dark blue to gray as it passed different redox states.

One particularly interesting and promising design for ECDs is dual electrochromic. Dual electrochromic ECDs based on PANI and polyaniline (PASA) are investigated in this thesis. The PANI/PASA thin film showed superior spectroelectrochemical properties compare to other ECDs reported here or elsewhere.

An electrode with single wall carbon nanotubes (SWCNTs) coating was tested as the substrate for an ECD based on poly[2-(3-thienyl) ethoxy-4-butylsulfonate] (PTEBS) to examine performance of the electrochromic polymer on a substrate other than an indium tin oxide (ITO) electrode. Compared to ITO, the SWCNT based device exhibited superior properties.

Acknowledgements

My highest appreciation and gratitude go to my wonderful advisor and mentor, Professor James R. Heflin. I cannot put in words my deepest appreciation for his help, support, guidance, patience and encouragement. Working under supervision of Professor Heflin was, and still is for my PhD, one of the best opportunities I have had in my entire life. I have learned a lot from his astounding knowledge in Physics and Materials Science. In addition to academic education, working for Professor Heflin has thought me very valuable lessons in my personal life. I feel I have learned a lot and improved a lot since the time I joined Professor Heflin's group in 2005 as an undergraduate Physics student; and I am very thankful for it. I am indebted forever for his care, support and guidance.

I would also like to thank Professor Donald Leo at Mechanical Engineering department for his excellent guidance. I learned a lot from Professor Leo, but the most important lesson I learned from him is the time management. I am astonished how Professor Leo does so much work and is always full of energy, smiling, positive and has time to meet with me. I would also like to express my gratitude to Professor Abby W. Morgan for her generous help, advice, and support.

In addition to my committee members, I would also like to thank Professor Karen Depauw, the dean of the Graduate School, who change the way I see to world. I am very appreciative of Professor David Clark, the head of the MSE department for giving me the opportunity to join this wonderful program. I would also like to express my gratitude to Professor John Simonetti at Physics department, whom I learned a lot from. I would also like to thank Mr. Stephen McCartney at ICTAS for his generous help.

Special thanks go to my beloved soul mate and my better half, Nastaran Hashemi. Thank you for being there with me during all the hard times in my academic life and personal life; I certainly owe you a lot, and hope that I can make it up to you some day.

I would also like to thank my parents for their unconditional love and support, I am very grateful for what they have done for me.

Thanks also go to my colleagues and friends Vaibhav Jain, Jason Ridley and Manpreet Kaur for very helpful discussions we had, and also to my very good friends Rodi, Sanaz, Mohammad, Parastoo, Parhum, Bitra and Bijan for being there at the most stressful times.

Table of Contents

Preface	i
<i>Abstract</i>	ii
<i>Acknowledgment</i>	iii
<i>Table of Contents</i>	iv
<i>List of Figures and Tables</i>	vi
Chapter 1. Introduction	1
1.1 <i>Background</i>	1
1.2 <i>Layer-by-layer Assembly</i>	2
1.2.1 <i>Assembly concept</i>	2
1.2.2 <i>Controlled Assembly</i>	3
1.3 <i>Electrochromism</i>	5
1.3.1 <i>Coloration</i>	5
1.4 <i>Electrochromic Devices</i>	6
1.4.1 <i>Single Electrochrome ECDs</i>	7
1.4.2 <i>Dual Electrochrome ECDs</i>	8
1.5 <i>Characterization Techniques and Methods</i>	8
1.5.1 <i>Cyclic Voltammetry</i>	8
1.5.2 <i>UV-Vis Spectroscopy</i>	9
1.5.3 <i>Square Wave Switching and Response Time</i>	11
1.6 <i>References</i>	12
Chapter 2. Single Electrochrome ECD Based on PEDOT LbL Thin Films	16
2.1 <i>Abstract</i>	16
2.2 <i>Introduction</i>	16
2.3 <i>Materials and Methods</i>	17
2.4 <i>Results and Discussions</i>	19
2.5 <i>Conclusion</i>	21
2.6 <i>References</i>	23
Chapter 3. Single Electrochrome ECD Based on PASA LbL Thin Films	24
3.1 <i>Abstract</i>	24
3.2 <i>Introduction</i>	24
3.3 <i>Materials and Methods</i>	26

3.3.1 Substrate	26
3.3.2 Solutions.....	26
3.3.3 Film Deposition	26
3.4 Results and Discussions	27
3.4.1 Cyclic Voltammetry.....	27
3.4.2 Color Change.....	28
3.4.3 Spectroelectrochemistry	29
3.5 Conclusion	30
3.6 References	31
Chapter 4. Dual Electrochromic ECD Based on PANI and PASA Thin Films	33
4.1 Abstract	33
4.2 Introduction.....	33
4.3 Materials and Methods	35
4.4 Results and Discussions	36
4.4.1 Thickness.....	36
4.4.2 Cyclic Voltammetry.....	38
4.4.3 Contrast	40
4.4.4 Switching Speed	43
4.4.5 Lifespan.....	45
4.5 Conclusion	45
4.6 References	47
Chapter 5. Highly Conductive and Transparent CNT Based Electrode for ECDs	49
5.1 Abstract	49
5.2 Introduction.....	49
5.3 Materials and Methods	51
5.4 Results and Discussions	51
5.5 Conclusion	57
5.6 References	58
Chapter 6. Conclusions and Recommendations	59

List of Figures and Tables

Figure 1-1: Formation of two bilayers of ionic polymers via LbL assembly technique	3
Figure 1-2: Schematic of LbL process	4
Figure 1-3: Schematic of globular conformation of a polymer chain with low charge density (right) is shown in comparison with a polymer chain with high charge density (left). Polymer chains with lower charge density form globular conformations and so thicker layers	5
Figure 1-4: Schematic of a liquid cell testing setup	7
Figure 1-5: Schematic of solid state, dual electrochromic ECD	7
Figure 1-6: Schematic of optical switching speed measuring setup	11
Figure 2-1: Percentage transmission vs wavelength of an electrochromic device consisting of two PAH/PEDOT 80 bilayer films with 2.0 and 0 V applied	18
Figure 2-2: Photodiode signal vs time with square wave voltage applied for a device consisting of two 40 bilayer films with 1 cm ² area	19
Figure 2-3: Decoloration (a) and coloration (b) of a 0.6 cm ² device consisting of two 40 bilayer PAH/PEDOT films with applied voltage of 0–1.4 V.	20
Figure 2-4: Decoloration and coloration switching times vs electrochromic device area for devices consisting of two 40 bilayer PEDOT films. Lines shown to guide the eye	21
Figure 3-1: LbL assembly technique. Layers of oppositely charged polymers are used to construct the thin polymer film	25
Figure 3-2: SEM image of 40 bilayers of PAH / PASA on ITO	27
Figure 3-3: Cyclic Voltammetry of (PAH/PASA) ₄₀ at 25, 50 and 100 mV/s scan rates. A reduction peak was observed at ~ +0.3 V and oxidation peaks at ~0 V and ~-0.6 V. The arrow indicates increasing scan rate	28
Figure 3-4: Color of (PAH/PASA) ₄₀ at different redox states. From left to right, oxidized, neutral and reduced	29
Figure 3-5: Transmittance of (PAH/PASA) ₄₀ at neutral and redox states. The highest contrast is about 30% and was observed at ~ 690 nm	30
Figure 4-1: Film thickness of PANI/PASA LbL films versus number of bilayers. The curve is an exponential fit to the data	37
Figure 4-2: The change in transmittance between +2.3 V and -2.3 V of PANI/PASA devices with different numbers of bilayers for 10 to 60 bilayers with 10 bilayers intervals. The arrow indicates increasing number of bilayers	37
Figure 4-3: Cyclic voltammograms of (PAH/PASA) ₄₀ taken at 25, 50, and 100 mV/s scan rates. The increasing total area under the curve corresponds to increasing scan rate	38

Figure 4-4: Cyclic voltammograms of (PANI/PAMPS) ₄₀ taken at 25, 50, and 100 mV/s scan rates. The increasing total area under the curve corresponds to increasing scan rate	39
Figure 4-5: Cyclic voltammogram of (PANI/PASA) ₄₀ taken at 25, 50, and 100 mV/s scan rates. The increasing total area under the curve corresponds to increasing scan rate. At higher scan rate the contribution of PASA is more obvious	40
Figure 4-6: Spectra of (PANI/PASA) ₄₀ asymmetric EC device taken from -2.5 V to +2.5 V at 0.5 V intervals. Dashed line indicates 0 V data, and the arrow indicates increasing potential	41
Figure 4-7: Spectra of (PANI/PASA) ₄₀ asymmetric EC device taken at -2.3, 0, and +2.3 V. The dashed line indicates the change in transmittance between -2.3 V spectra and +2.3 V spectra. Arrow indicates increasing potential	41
Figure 4-8: Spectra of (PAH/PASA) ₄₀ asymmetric EC device taken at -2.3, 0, and +2.3 V. The bold solid line indicates the 0 V spectrum, and the dashed line indicates the change in transmittance between -2.3 V spectra and +2.3 V spectra. The arrow indicates increasing potential	42
Figure 4-9: Spectra of (PANI/PAMPS) ₄₀ asymmetric EC device taken at -2.3, 0, and +2.3 V. The dashed line indicates the change in transmittance between -2.3 V spectra and +2.3 V spectra. Arrow indicates increasing potential	43
Figure 4-10: Switching speed response of (PANI/PASA) ₄₀ asymmetric EC device during application of +/- 2.3 V square wave at 0.25 Hz	44
Figure 4-11: Switching speed response of (PANI/PAMPS) ₄₀ asymmetric EC device during application of +/- 2.3 V square wave at 0.25 Hz	44
Figure 4-12: Spectra of (PANI/PASA) ₄₀ taken at -2.3 V and + 2.3V, before (solid line) and after (dotted line) going through more than 1000 switching cycles	45
Figure 5-1: Scanning electron microscopy images of CNT electrode with (a) no film, (b) two bilayers, (c) five bilayers, and (d) ten bilayers of PAH/PTEBS film	52
Figure 5-2: AFM height images of bare CNT electrode and film with two, five, eight, and ten bilayers. Area is 2×2 μm ² and the z scale is from 0 to 60 nm. Also represented is the average surface roughness plot for different numbers of bilayers	54
Figure 5-3: (a) CV of the bare CNT electrode at 10 mV/s and 40-bilayer film of PAH/PTEBS at 5, 10, 15, and 20 mV/s. (b) The linear relationship of peak current with the square root of scan rate	55
Figure 5-4: Change in transmission spectra of 40-bilayer PAH/PTEBS film on application of 0 V and step increase in voltage from 0.75 to 2.0 V	57
Table 6-1: Summary of the characteristics and properties of the ECDs discussed in this thesis	61

Chapter 1: Introduction

1.1 Background

Engineering and development of functional devices based on discoveries in pure science requires a good understanding of both science and engineering, very often in more than one discipline. Multidisciplinary research in science and engineering contributes to advancements in both areas. Scientific foundations and discoveries are applied to engineer applications through multidisciplinary research. Also, in the development of engineering applications many scientific facts have been discovered. Both science and engineering were applied to design, fabricate and analyze the devices proposed in this thesis.

This thesis is focused on the development of electrochromic devices, which change color and or opacity in response to an applied voltage. Improvements in the morphology of the thin films and design of the electrochromic devices are achieved and reported. Improvement of the contrast and switching speed of electrochromic devices is the main goal of this thesis and it is achieved via choice of materials, optimization of the morphology and structure of the thin film as well as the design of the electrochromic device. The results were studied and analyzed by a variety of tools and techniques such as cyclic voltammetry and optical switching speed measurements.

For fabrication of the thin films, the layer-by-layer (LbL) assembly technique was used, which allows control over several critical factors for fabrication of the thin films such as control over the thickness of the thin film and morphology of it. In most of the work, the thin films were fabricated on indium tin oxide (ITO) coated glass electrodes because of the high transparency and high conductivity of ITO coatings. In one of the studies, in order to improve the quality of the electrodes, glass slides coated with carbon nanotubes were also fabricated and tested in comparison to ITO coated electrodes.

Electrochromic devices based on electrochromic polymers were fabricated and tested and exhibited high contrast and fast switching speed. Electrochromic devices with two electrochromic polymers (dual electrochrome) was also fabricated and studied.

This thesis explores different aspects of the electrochromic properties of solid state electrochromic devices and electrochromic polymers fabricated using the LbL technique to achieve highly homogeneous films with nanoscale control of the thickness.

1.2 Layer-by-layer Assembly

Fabrication of functional thin films can be achieved via several deposition techniques including physical or chemical vapor deposition, electroplating, spin assisted or spray coating, layer-by-layer (LbL) deposition, and several other techniques. Among all the techniques mentioned above, LbL has several significant advantages that make this technique very useful for fabrication of functional thin films. One key feature of the LbL technique is that any species with multiple ionic charges can be used as one of the components of the LbL assembled thin films¹. This phenomenon, along with the fact that charged species can be deposited from aqueous solutions, make a wide range of materials available to be used with this technique such as ionic polymers²⁻⁴, nano-particles⁵⁻⁷, dendrimers⁸⁻¹⁰, quantum dots¹¹⁻¹³, proteins¹⁴⁻¹⁵, and DNA¹⁶⁻¹⁷.

The LbL assembly technique was first developed and introduced in 1966 by Iler¹⁸ at Dupont. The technique did not receive much credit nor attention from the scientific community until it was reintroduced in 1991 by Decher *et al*¹⁹ as a solution for deposition of charged polymers. Since its redevelopment in 1991, the LbL assembly technique has become one of the most preferred techniques for fabrication of thin films and has been practiced by numerous research groups worldwide. The LbL assembly technique is used for fabrication of all the electrochromic thin films investigated in this thesis.

1.2.1 Assembly Concept

The LbL assembly technique is based on sequential deposition of oppositely charged species on a charged substrate^{18, 20-22}. Although different types of chemical bonds may be involved in formation of the multilayer thin films²³⁻²⁴, the most common form of LbL deposition is based on ionic bonds between ionic species^{1, 22}. Figure 1-1 shows a schematic of formation of two bilayer via ionic attraction between two ionic polymers.

Exposure of the charged substrate to a dilute aqueous ionic solution of opposite charge forms an ultra thin layer of the charged molecules on the surface of the substrate. The substrate is then rinsed with deionized (DI) water to wash the loosely bound molecules and immersed in the other dilute aqueous ionic solution with a charge opposite to the charge of the first ionic solution to form another ultra thin film on the top of the existing, first, ultrathin film. This step is also followed by rinsing with DI water. The two-layer system forms one bilayer. Repetition of these

steps results in formation of thin films consisting of several bilayers. A schematic of the LbL assembly process is shown in Figure 1-2.

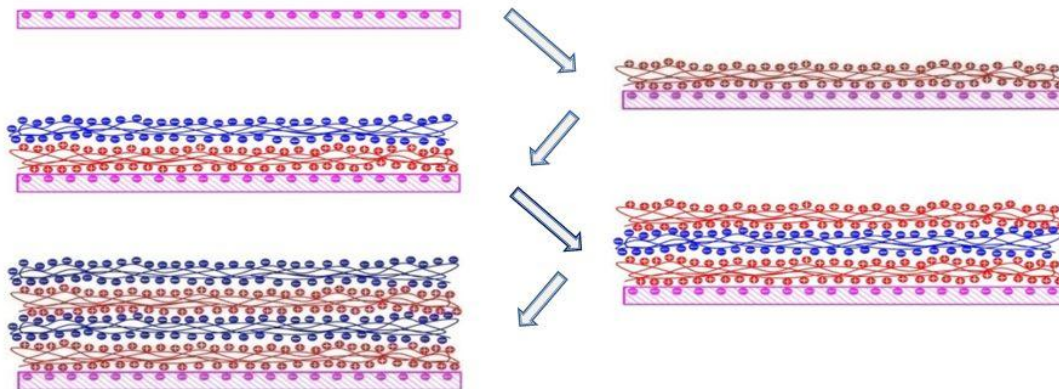


Figure 1-1. Formation of two bilayers of ionic polymers via LbL assembly technique.

Although a wide range of charged materials can be used in the LbL assembly technique, as mentioned in section 1.2, only ionic polymers (polycations and polyanions) are used for fabrication of all thin films investigated in this thesis.

1.2.2 Controlled Assembly

Control over the thickness and morphology of each bilayer, and the thin film as a whole, is significantly important in characterization and performance of the functional thin films. The LbL assembly technique can be adopted to fabricate thin films of a variety of properties. The morphology and properties of the bilayers can be determined by conditions of the deposition process and characteristics of the ionic species. Deposition conditions such as dipping duration and number of bilayers, along with solution characteristics such as pH,²⁵⁻²⁶ ion concentration,²⁷ ion type²⁸, ion strength,²⁹ and molecular weight²⁸ can influence the composition of the thin films.

Adjusting and optimizing these factors can manipulate the thin films to have desired properties. The dipping duration can vary from 1 to approximately 30 minutes. After a certain amount of time, depending on the conditions and materials, the deposition rate approaches zero due to charge balance between the existing and depositing layers and repulsion of the outer layer towards the polymers in solution. The charge strength of the materials also effects the deposition quality significantly³⁰⁻³².



Figure 1-2. Schematic of LbL process.

In the case of ionic polymers, varying the charge density of the polymer backbone chains also influence the morphology and the thickness of the thin films. Normally, the polymer molecules are in the form of long chains and the ionic charge is homogeneously distributed along them. Addition of counterions, usually through addition of salt, neutralizes some fraction of the charges and reduces the repulsion force along the polymer chain; following the lack of enough repulsion force, the polymer chains curl and form cluster conformations³³⁻³⁵. As shown in Figure 1-3, layers deposited from such solutions are generally thicker due to globular arrangement of the polymer molecules.

Another way to manipulate the charge on the polymer backbone is to adjust the pH of the solution^{27, 36-38}. This method is especially useful for cases in which the electrolyte is weak, which means that it can be neutralized near neutral pH. Increasing or decreasing the pH increases the charge of carboxyl or amine groups respectively³⁹⁻⁴². Polyanions are fully charged at high pH and polycations are fully charged at low pH.

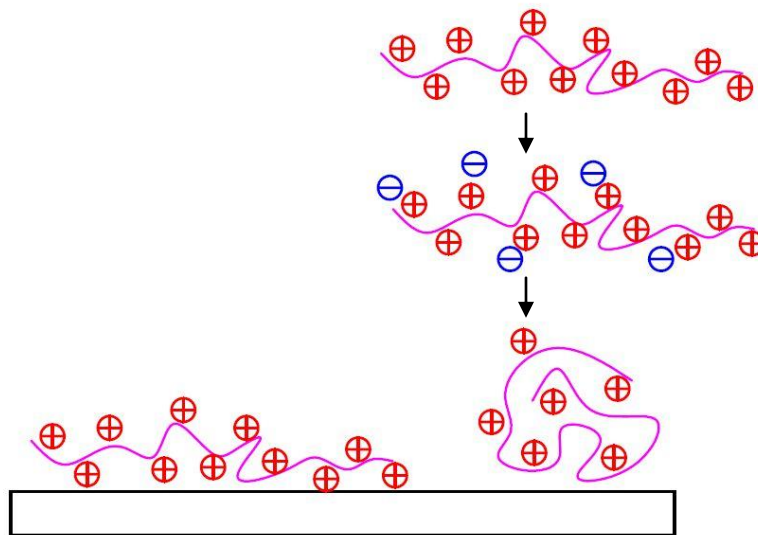


Figure 1-3. Schematic of globular conformation of a polymer chain with low charge density (right) is shown in comparison with a polymer chain with high charge density (left). Polymer chains with lower charge density form globular conformations and so thicker layers.

1.3 Electrochromism

The color of any material that does not itself emit light correlates to the wavelength of the reflected or transmitted portion of the incident light (depending on whether the material is viewed in reflection or transmission), which correlate to the absorbed portion of the incident light. As a result, materials that absorb shorter wavelengths appear red-orange whereas materials absorbing longer wavelengths appear blue-purple.

The molecules in a material absorb energy in discrete amounts corresponding to the absorbed wavelength, and the energy is consumed by intermolecular or intramolecular processes. The intensity of the reflected light is equal to the total intensity of the incident light minus the intensity of the absorbed and transmitted light.

1.3.1 Coloration

The change in the chemical structure of materials results in changes in their properties, one of which may be a change in the optical density spectrum. This change causes the materials to appear a different color.⁴³⁻⁴⁵

If the change in the chemical structure occurs due to the application of an electric field, the

phenomenon is termed “electrochromism”. Polymers with this characteristic are termed “electrochromic polymers”.

The most sought-after electrochromic materials are ones capable of undergoing reversible electrochromism, exhibiting dramatic color change (high contrast) usually from almost fully transparent to almost fully opaque in a short period of time (fast switching speed)

1.4 Electrochromic Devices

Integration of electrochromic materials into devices makes it possible to take advantage of such materials in practical ways and makes it easier to define standards when investigating the characteristics of the electrochromic materials.⁴⁴ It is through electrochromic devices (ECDs) that optimization of the electrochromic materials become possible.⁴⁵⁻⁴⁷

The most practical design for testing and commercializing electrochromic devices is the solid-state design.⁴⁸⁻⁵¹ However, electrochromic thin films can operate in electrochemical cuvettes as well^{3, 52}. The electrochemical cuvette setup is more suitable for testing the materials in a laboratory setting where functionality of the materials is the highest priority vs. the practicality. As shown in Figure 1-4, in this setting, the coated electrode is immersed in electrolyte solution along with a counter electrode, usually copper. The electric field is applied across the electrodes. Based on the magnitude and polarity of the electric field, the thin film undergoes redox reactions in its interaction with the electrolyte. Due to the involvement of a large volume of electrolytes and the design of this setting, liquid cell setting is not appropriate for commercial usage.

A solid-state electrochromic device typically consists of two ITO glass electrodes at least one of which is coated with a thin film. The counter electrode can be an uncoated ITO glass electrode, one with identical thin film, or one with a different type of thin film. A very thin layer of electrolyte gel is usually placed between the two electrodes. The thickness of the electrolyte layer can be determined by use of spacers. A schematic of a solid-state electrochromic device is shown in Figure 1-5. The device can be sealed by tape, epoxy, or other types of sealant to prevent leakage of the electrolyte gel and promote ease of handling of the device.

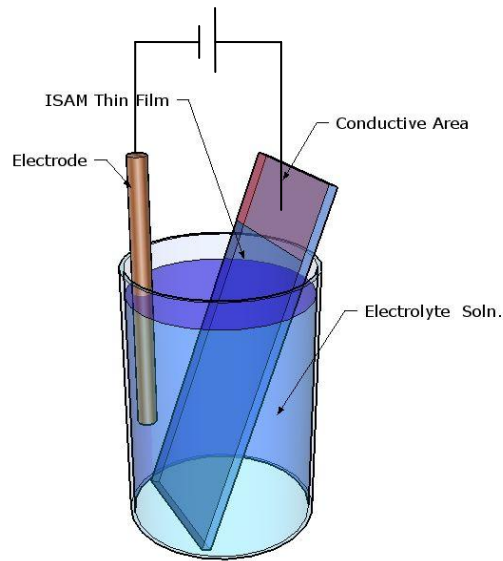


Figure 1-4. Schematic of a liquid cell testing setup

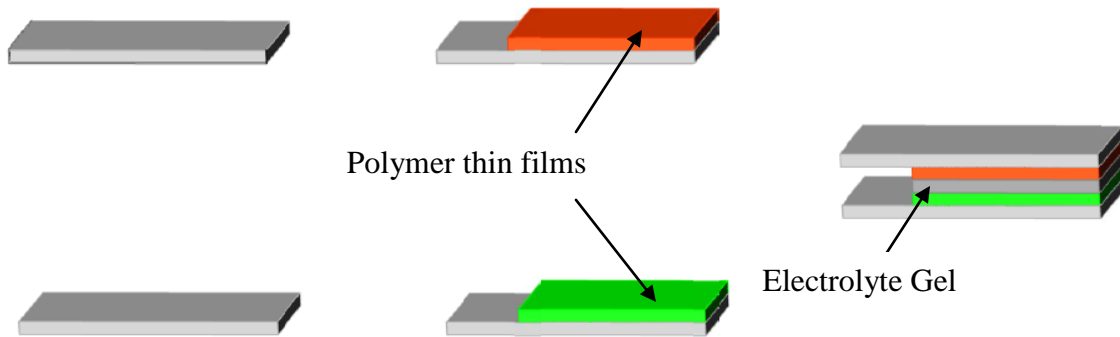


Figure 1-5. Schematic of solid state, dual electrochromic ECD

1.4.1 Single Electrochromic ECDs

As mentioned in section 1.2.1, at least two ionic species are required to form a set of bilayers, one polycation and one polyanion. In the case of electrochromic devices, at least one of the two ionic species must have electrochromic properties, i.e. be electrochromically active.

Devices with only one electrochromic species are called single electrochromic electrochromic devices. Such devices may have less redox states compared to devices consisting of more than one electrochromically active species.

The cyclic voltammetry (CV) plots of single electrochromic ECDs are easier to analyze, and transmittance of the device in the neutral state (no electric field applied) is higher. The reason for higher transmittance in the neutral state is that the electrochemically inactive materials are chosen among colorless materials whereas most electrochromically active materials are colored.

Poly(allylamine hydrochloride) (PAH) (polycation), poly (2-acrylamido 2-methyl propane sulfonic acid) (PAMPS) (polyanion) and poly(acrylic acid) (PAA) (polyanion) are among widely used, colorless, electrochromically inactive polymers.

The properties of electrochemically active polymers are discussed in detail in the following chapters.

1.4.2 Dual Electrochromic ECDs

Dual electrochromic electrochromic devices consist of two electrochromically active materials.⁵²⁻⁵³ Having two electrochromically active materials in one system adds to the complexity of the system; however, there are several advantages associated with such systems that are rare in single electrochromic ECDs. One advantage is the possibility of having several color changes in a small electric potential window. The other advantage of dual electrochromic ECDs is that the entire thin film is contributing to the electrochromism of the device, versus in single electrochromic ECDs only a portion of the thin film is electrochromically active.

1.5 Characterization Techniques and Methods

Electrochemical analyses are important in gaining a better understanding of the compositional details of the thin films. There have been several methods and techniques for performing controlled electrochemical reactions, some of which are more common than others. Electrochemical processes are either voltammetric or amperometric; due to the very small amount of materials, voltammetric processes are preferred for analyzing the thin films. Voltammetric electrochemical analyses are performed for all the thin films investigated in this thesis.

1.5.1 Cyclic Voltammetry

Cyclic voltammetry (CV) is a very common potentiodynamic electrochemical measurement technique, widely used to investigate and describe electrochemical properties of an electrical

conductive system. Most of the new electrochromic materials and composites are subject to CV for determination of their general electrochemical nature. The redox potentials of a system can also be interpreted from the CV data.

In classical CV, the potential across the working electrode, i.e. the sample, and a counter electrode is swept linearly between an upper and lower limit. The potential window should include the potentials at which the redox states are expected. The current passing through the working electrode is continuously measured and recorded with respect to a reference electrode. Data are usually represented as current vs. voltage plots. Redox potentials are identified from the position of the oxidation and reduction current peaks. Current peaks represent the potentials at which the reaction rate between the working electrode and the electrolyte environment is the greatest.

In classical CV, the reaction between working electrode and the environment is either *activation*, also known as charge transfer, or *diffusion*, also known as mass transfer, controlled. The reaction type can be determined by studying the position of the current peaks at different scan rates. Change in the magnitude of the current peaks in activation controlled reactions shows a linear response to the change of the scan rate whereas diffusion controlled reactions exhibit a nonlinear response.

One other attribute of diffusion controlled reactions is the shift in the position of the current peaks at different scan rates. The current peaks shift away from the zero potential point as the scan rate increases. The reason for the shift is the lag in time between the potential reading and the reaction occurrence.

In the case of thin films, activation controlled reaction will occur when the thin film consists of only one monolayer, for example. In this case, the whole reaction is taking place at the surface where there is no separation between the electrode surface and the reaction zone. As the thickness of the thin film goes beyond one monolayer, the reaction, to some extent, becomes diffusion controlled. As the thickness increases the signs of diffusion controlled reaction become more obvious.

1.5.2 UV-Vis Spectroscopy

In this method, the optical properties of the thin film at a fixed potential is studied as a function of the wavelength of the incident light. The method involves the passage of a collimated

light beam of a varying wavelength (visible spectrum in this case) through the electrochromic device. The intensity of the transmitted light is then measured and recorded as a function of the wavelength.

There are several ways to represent and interpret the collected data; the most common ways are percent transmittance (%T) and absorbance (A). Absorbance and percent transmittance are related by

$$A = \log_{10} \left(\frac{100}{\%T} \right) = -\log_{10} T \quad \text{Eqn. 1}$$

The thickness of the thin film can be calculated from a model based on the Beer-Lambert equation, which is a more detailed version of the above equation.

$$\epsilon lc = \log_{10} \frac{100}{\%T} \quad \text{Eqn. 2}$$

where ϵ is the molar absorptivity, c is the concentration of the electrochromic species, and l is the path length or thickness of the thin film. Absorptivity and concentration values are based on intrinsic properties of any material and are independent of the composition of the thin film. The values of these constants can be looked up from a table where available or can be calculated from the absorbance of samples with known thicknesses. The calculated value, k , (where $k = \epsilon c$) can be used in calculating the thickness of the thin films from the absorbance intensity. Equation 3 can be rewritten as:

$$kl = \log \frac{100}{\%T} = A \quad \rightarrow \quad l = \frac{A}{k} \quad \text{Eqn. 3}$$

The intensity of the reflected light from the thin film can also be calculated with UV-Vis spectroscopy technique using the basic phenomenon that the total intensity of the transmitted, absorbed, and reflected lights are equal to the intensity of the incident light. However, since the intensity of the scattered light is not distinguished from the intensity of the reflected light, the calculated intensity of reflected light is actually the sum of these two intensities.

1.5.3 Square Wave Switching and Response Time

Square wave switching provides detailed information about the electric charge capacitance of the thin film. The information can be used in characterizing the thin film, mainly the optical switching speed that is especially important when evaluating the performance of electrochromic devices. Electrochromic devices with fast switching speed are needed in systems such as video displays and optical switching devices. The time required for the polymer to go from one redox state to another is the limiting factor for switching speed.

In this method, the potential at the device is alternated between the complete oxidation and complete reduction potentials for several cycles, forcing the materials through its redox states at the pace of the frequency of the square wave.

Since all the polymers investigated in this thesis are electrochromic polymers used in ECDs, the optical switching speed was directly measured from the color change of the ECDs. In this method, a beam of laser is passed through the ECD during the square wave switching; the change in the intensity of the laser is detected using a photodiode, and carefully studied in reference to the square wave to determine the time required for the polymer to alternate between redox states. Figure 1-6 shows the schematic of the setup used in measuring the optical switching speed.

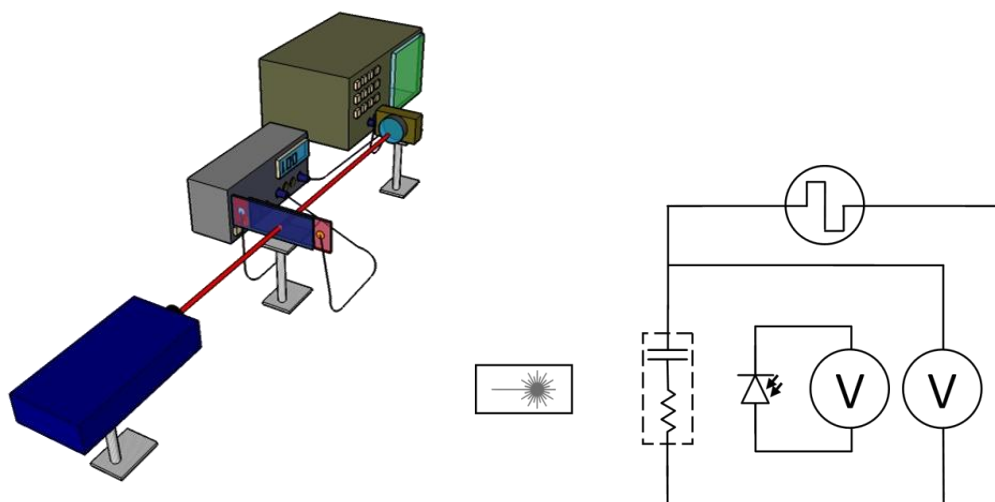


Figure 1-6. Schematic of optical switching speed measuring setup

1.6 References

1. Lutkenhaus, J. L.; Hammond, P. T., *Electrochemically enabled polyelectrolyte multilayer devices: from fuel cells to sensors*. *Soft Matter* 2007, 3, (7), 804-816.
2. Stroeve, P.; Vasquez, V.; Coelho, M.; Rabolt, J., *Gas transfer in supported films made by molecular self-assembly of ionic polymers*. *THIN SOLID FILMS* 1996, 284, 708-712.
3. Jain, V.; Yochum, H.; Wang, H.; Montazami, R.; Hurtado, M. A. V.; Mendoza-Galvan, A.; Gibson, H. W.; Heflin, J. R., *Solid-state electrochromic devices via ionic self-assembled multilayers (ISAM) of a polyviologen*. *Macromolecular Chemistry and Physics* 2008, 209, (2), 150-157.
4. Jain, V.; Sahoo, R.; Jinschek, J. R.; Montazami, R.; Yochum, H. M.; Beyer, F. L.; Kumar, A.; Heflin, J. R., *High contrast solid state electrochromic devices based on Ruthenium Purple nanocomposites fabricated by layer-by-layer assembly*. *Chemical Communications* 2008, (31), 3663-3665.
5. Kotov, N. A.; Dekany, I.; Fendler, J. H., *Layer-by-Layer Self-Assembly of Polyelectrolyte-Semiconductor Nanoparticle Composite Films*. *The Journal of Physical Chemistry* 2002, 99, (35), 13065-13069.
6. Malikova, N.; Pastoriza-Santos, I.; Schierhorn, M.; Kotov, N.; Liz-Marzan, L., *Layer-by-layer assembled mixed spherical and planar gold nanoparticles: control of interparticle interactions*. *LANGMUIR* 2002, 18, (9), 3694-3697.
7. Mamedov, A.; Kotov, N., *Free-standing layer-by-layer assembled films of magnetite nanoparticles*. *LANGMUIR* 2000, 16, (13), 5530-5533.
8. Anzai, J.; Kobayashi, Y.; Nakamura, N.; Nishimura, M.; Hoshi, T., *Layer-by-layer construction of multilayer thin films composed of avidin and biotin-labeled poly (amine) s*. *LANGMUIR* 1999, 15, (1), 221-226.
9. Aroca, R.; Goulet, P.; DOS SANTOS, D.; Alvarez-Puebla, R.; OLIVEIRA, O., *Silver nanowire layer-by-layer films as substrates for surface-enhanced Raman scattering*. *Analytical chemistry*(Washington, DC) 2005, 77, (2), 378-382.
10. Crespilho, F.; Huguenin, F.; Zucolotto, V.; Olivi, P.; Nart, F.; Oliveira, O., *Dendrimers as nanoreactors to produce platinum nanoparticles embedded in layer-by-layer films for methanol-tolerant cathodes*. *ELECTROCHEMISTRY COMMUNICATIONS* 2006, 8, (2), 348-352.
11. Jaffar, S.; Nam, K.; Khademhosseini, A.; Xing, J.; Langer, R.; Belcher, A., *Layer-by-layer surface modification and patterned electrostatic deposition of quantum dots*. *NANO LETTERS* 2004, 4, (8), 1421-1426.
12. Constantine, C.; Gattas-Asfura, K.; Mello, S.; Crespo, G.; Rastogi, V.; Cheng, T.; DeFrank, J.; Leblanc, R., *Layer-by-layer films of chitosan, organophosphorus hydrolase and thioglycolic acid-capped CdSe quantum dots for the detection of paraoxon*. *J. Phys. Chem. B* 2003, 107, (50), 13762-13764.
13. Sarathy, K.; Thomas, P.; Kulkarni, G.; Rao, C., *Superlattices of Metal and Metal-Semiconductor Quantum Dots Obtained by Layer-by-Layer Deposition of Nanoparticle Arrays*. *J. Phys. Chem. B* 1999, 103, (3), 399-401.
14. Hong, J.; Lowack, K.; Schmidt, J.; Decher, G., *Layer-by-layer deposited multilayer assemblies of polyelectrolytes and proteins: from ultrathin films to protein arrays*. *PROGRESS IN COLLOID AND POLYMER SCIENCE* 1993, 93, 98-98.

15. Cassier, T.; Lowack, K.; Decher, G., *Layer-by-layer assembled protein/polymer hybrid films: nanoconstruction via specific recognition. Supramolecular Science* 1998, 5, (3-4), 309-315.
16. Lang, J.; Liu, M., *Layer-by-layer assembly of DNA films and their interactions with dyes. J. Phys. Chem. B* 1999, 103, (51), 11393-11397.
17. Lu, L.; Wang, S.; Lin, X., *Fabrication of layer-by-layer deposited multilayer films containing DNA and gold nanoparticle for norepinephrine biosensor. Analytica chimica acta* 2004, 519, (2), 161-166.
18. Iller, R. K., *Multilayers of colloidal particles. Journal of Colloid and Interface Science* 1966, 21, 569-594.
19. Decher, G. H., J.D., *Buildup of ultrathin multilayer films by a self-assembly process 1. Consecutive adsorption of anionic and cationic bipolar amphiphiles on charged surfaces. Macromol. Chem., Macromol. Symp* 1991, 46, 231.
20. Decher, G.; Eckle, M.; Schmitt, J.; Struth, B., *Layer-by-layer assembled multicomposite films. Current Opinion in Colloid & Interface Science* 1998, 3, 32-39.
21. Decher, G., *Fuzzy Nanoassemblies: Toward Layered Polymeric Multicomposites. Science* 1997, 277, (5330), 1232-1237.
22. Decher, G.; Hong, J. D.; Schmitt, J., *Buildup of ultrathin multilayer films by a self-assembly process: III. Consecutively alternating adsorption of anionic and cationic polyelectrolytes on charged surfaces. THIN SOLID FILMS* 1992, 210-211, (Part 2), 831-835.
23. Stockton, W. B.; Rubner, M. F., *Molecular-Level Processing of Conjugated Polymers. 4. Layer-by-Layer Manipulation of Polyaniline via Hydrogen-Bonding Interactions. MACROMOLECULES* 1997, 30, (9), 2717-2725.
24. Sukhishvili, S. A.; Granick, S., *Layered, Erasable, Ultrathin Polymer Films. JOURNAL OF THE AMERICAN CHEMICAL SOCIETY* 2000, 122, (39), 9550-9551.
25. Rubner, M., *pH-Controlled fabrication of polyelectrolyte multilayers: Assembly and applications. Multilayer thin films: sequential assembly of nanocomposite materials* 2003, 133.
26. Shiratori, S.; Rubner, M., *pH-dependent thickness behavior of sequentially adsorbed layers of weak polyelectrolytes. MACROMOLECULES* 2000, 33, (11), 4213-4219.
27. Bungenberg de Jong, H., *Crystallisation-coacervation-flocculation. Colloid Science* 1949, 2, 232-255.
28. Clark, S. L.; Montague, M.; Hammond, P. T., *Selective deposition in multilayer assembly: SAMs as molecular templates. Supramolecular Science* 1997, 4, (1-2), 141-146.
29. Clark, S.; Montague, M.; Hammond, P., *Templating of Layer-by-Layer Thin Films: Use of Surface Functionality to Direct Polyion Deposition. POLYMERIC MATERIALS SCIENCE AND ENGINEERING-WASHINGTON-* 1997, 77, 620-621.
30. Lvov, Y.; Decher, G.; Moehwald, H., *Assembly, structural characterization, and thermal behavior of layer-by-layer deposited ultrathin films of poly (vinyl sulfate) and poly (allylamine). LANGMUIR* 1993, 9, (2), 481-486.
31. Krozer, A.; Nordin, S.; Kasemo, B., *Layer by Layer Deposition of 5–50-nm Colloidal Silica Particles Studied by Quartz Microbalance. Journal of Colloid and Interface Science* 1995, 176, (2), 479-484.

32. Xie, A.; Granick, S., *Local electrostatics within a polyelectrolyte multilayer with embedded weak polyelectrolyte*. *Macromolecules* 2002, 35, 1805-1813.
33. Van de Steeg, H.; Cohen Stuart, M.; De Keizer, A.; Bijsterbosch, B., *Polyelectrolyte adsorption: a subtle balance of forces*. *LANGMUIR* 1992, 8, (10), 2538-2546.
34. Bonekamp, B. C.; Vanderschee, H. A.; Lyklema, J., *Journal of Croatica Chemica Acta* 1983, 56, 695-704.
35. Stuart, M. A. C.; Tamai, H., *Dynamics of adsorbed polymers. 2. Thickness relaxation of poly (ethylene oxide) on glass as a function of segmental binding energy*. *LANGMUIR* 1988, 4, (5), 1184-1188.
36. Yoo, D.; Shiratori, S.; Rubner, M., *Controlling bilayer composition and surface wettability of sequentially adsorbed multilayers of weak polyelectrolytes*. *MACROMOLECULES* 1998, 31, (13), 4309-4318.
37. Shiratori, S. S.; Rubner, M. F., *pH-Dependent Thickness Behavior of Sequentially Adsorbed Layers of Weak Polyelectrolytes*. *MACROMOLECULES* 2000, 33, (11), 4213-4219.
38. Dubas, S.; Schlenoff, J., *Polyelectrolyte multilayers containing a weak polyacid: construction and deconstruction*. *MACROMOLECULES* 2001, 34, (11), 3736-3740.
39. Bohmer, M.; Evers, O.; Scheutjens, J., *Weak polyelectrolytes between two surfaces: adsorption and stabilization*. *MACROMOLECULES* 1990, 23, (8), 2288-2301.
40. Blaakmeer, J.; Bohmer, M.; Stuart, M.; Fler, G., *Adsorption of weak polyelectrolytes on highly charged surfaces. Poly (acrylic acid) on polystyrene latex with strong cationic groups*. *MACROMOLECULES* 1990, 23, 2301-2309.
41. Böhmer, M.; El Attar Sofi, Y.; Foissy, A., *Calorimetry of Poly-(Acrylic Acid) Adsorption on TiO₂*. *Journal of Colloid and Interface Science* 1994, 164, 126-135.
42. Dupont, L.; Foissy, A., *Evaluation of the adsorption trends of a low molecular-weight polyelectrolyte with a site-binding model*. *Colloids and Surfaces A: Physicochemical and Engineering Aspects* 1996, 110, (3), 235-248.
43. Mortimer, R. J., *Electrochromic Materials Chemical Society Reviews* 1997, 26, 147-156.
44. Granqvist, C., *Electrochromic devices*. *Journal of the European Ceramic Society* 2005, 25, (12), 2907-2912.
45. Granqvist, C. G.; Avendaño, E.; Azens, A., *Electrochromic coatings and devices: survey of some recent advances*. *Thin Solid Films* 2003, 442, (1-2), 201-211.
46. Granqvist, C. G., *Electrochromic tungsten oxide films: review of progress 1993-1998*. *Solar Energy Materials and Solar Cells* 2001, 60, 201-262.
47. Granqvist, C. G., *Handbook of Inorganic Electrochromic Materials* 1995.
48. Kim, E.; Jung, S., *Layer-by-Layer Assembled Electrochromic Films for All-Solid-State Electrochromic Devices*. *Chemistry of Materials* 2005, 17, (25), 6381-6387.
49. Gratzel, M., *Materials science: Ultrafast colour displays*. *Nature* 2001, 409, (6820), 575-576.
50. Jung, S.; Kim, H.; Han, M.; Kang, Y.; Kim, E., *Layer-by-layer assembly of poly(aniline-N-butylsulfonate)s and their electrochromic properties in an all solid state window*. *Materials Science and Engineering: C* 2004, 24, (1-2), 57-60.
51. Kim, E.; Lee, K.; Rhee, S. B., *Electrochromic Window Based on Poly(aniline-N-butylsulfonate)s with a Radiation-Cured Solid Polymer Electrolyte Film*. *JOURNAL OF THE ELECTROCHEMICAL SOCIETY* 1997, 144, (1), 227-232.

52. DeLongchamp, D. M.; Kastantin, M.; Hammond, P. T., *High-contrast electrochromism from layer-by-layer polymer films. Chemistry of Materials* 2003, 15, (8), 1575-1586.
53. DeLongchamp, D. M.; Hammond, P. T., *Multiple-color electrochromism from layer-by-layer-assembled polyaniline/Prussian blue nanocomposite thin films. Chemistry of Materials* 2004, 16, (23), 4799-4805.

Chapter 2: Single Electrochromic ECD Based on PEDOT LbL Thin Film

Millisecond switching in solid state electrochromic polymer devices fabricated from ionic self-assembled multilayers

Published in Applied Physics Letters, 2008, 92

Authors: Jain, V.; Yochum, H.; Montazami, R.; Heflin, J.R.

2.1 Abstract

The electrochromic switching times of solid state conducting polymer devices fabricated by the ionic self-assembled multilayer method has been investigated. The devices were composed of bilayers of poly(3,4-ethylenedioxythiophene): poly(styrenesulfonate) and poly(allylamine hydrochloride) on indium tin oxide substrates. Devices fabricated from 40 bilayer thick films have coloration and decoloration switching times of 31 and 6 ms, respectively, with low applied voltage (1.4 V) for an active area of 0.6 cm². The switching times have been shown to decrease with the active area of the electrochromic device suggesting that even faster electrochromic switching times are possible for devices with smaller areas.

2.2 Introduction

Electrochromic (EC) devices show a reversible color change upon reduction or oxidation of the electrochromic material by application of a voltage. Tungsten oxide electrochromic devices have been used in smart windows, automotive rear-view mirrors, and thin passive displays for more than a decade, but electrochromic materials have not yet been employed in fast displays because of their slow color-switching response time, typically on the order of seconds. A large number of conducting polymers exhibit electrochromic behavior, including polyaniline, polyviologens, and polypyrrole, but poly(3,4-ethylenedioxythiophene):poly(styrenesulfonate) (PEDOT:PSS) has been preferred in electrochromic studies because of its easy processability, high conductivity (300 S/cm), high contrast at low voltage, and long term stability without degradation as compared to other conducting polymers.¹⁻⁴ Here, we demonstrate fast switching response time (<10 ms) of electrochromic devices consisting of PEDOT:PSS and poly(allylamine hydrochloride) (PAH) multilayered films fabricated by the ionic self-assembled multilayer (ISAM) approach.

The electrochromic properties of PEDOT:PSS have been studied by several groups. Delongchamp *et al.* fabricated solid state dual electrochromic PEDOT and polyaniline ISAM films which had switching speeds ($t_{75\%}$) of 0.37 s for decoloration and 1.22 s for coloration. Kumar *et al.* found that PEDOT:PSS films made by electropolymerization have switching speeds of several seconds for thicknesses of 300 nm.⁵ Cho *et al.* have shown that PEDOT nanotubes fabricated in an intricate process of laying out an array structure on indium tin oxide (ITO) with a silica template have very fast reflectivity changes of 8.8 ms coloration and 3.5 ms decoloration for nanotubes of 20 nm wall thickness with -1 V– $+1$ V applied for a reflectivity change of 25%.⁶ We report PEDOT electrochromic devices that operate at comparable switching rates as reported by Cho *et al.* and can be made with the fairly simple and inexpensive ISAM approach with readily available conducting electrodes and materials.

2.3 Materials and Methods

ISAM films are formed by a layer-by-layer deposition technique⁷ that provides highly precise, nanometer-scale films on the electrode surface. ISAM films have been used for a variety of applications,⁸ for example, in nonlinear optics,⁹⁻¹⁰ optical sensors,¹¹ light-emitting diodes,¹² and photovoltaics.¹³⁻¹⁴ ISAMs have also been used in the fabrication of a variety of electrochromic films, including PEDOT, but the PEDOT devices did not have the fast switching times reported here.² The ISAM technique allows the possibility of choosing a wide range of electrochromic materials that can be used in combination with PEDOT for dual and multihue electrochromic devices.¹

The ISAM technique involves dipping a charged substrate alternately in aqueous polycation and polyanion solutions. We have used glass slides coated with ITO as our substrate, PAH as the cationic polymer, and PEDOT:PSS as the anionic polymer. Symmetric solid state devices were fabricated by sandwiching together two ITO slides coated with PEDOT/PAH bilayers using a transparent conducting gel poly(2-acylamido 2-methyl propane sulfonic acid). The device structure is shown in the inset of Figure 2-1. We used 10 mM PAH (Sigma-Aldrich) at pH 4 and PEDOT:PSS (BaytronP) has been prepared by the method described by Delongchamp *et al.*¹ The area of the electrochromic device was controlled by appropriately etching the ITO substrates to create stripes or pixels of the desired size. Cyclic voltammetry, not shown here, of a (PAH/PEDOT:PSS)₄₀ film shows a broad reduction peak of the PEDOT and is consistent with

the measurements of Tang *et al.*³ The diffusion coefficient ($D_e \sim 2.82 \times 10^{-8}$ cm²/s) value calculated by the Randles-Sevcik equation,

$$I_p = (2.69 \times 10^5) n^{3/2} A D_e^{1/2} C \nu^{1/2}$$

where $I_p = 321$ mA is the cathodic peak current, $n = 1$ is the electron stoichiometry, $A = 1$ is the electrode area (cm²), $C = 0.01$ is the concentration of electrolyte (mol/cm³), $\nu = 0.5$ is the scan rate (V/s).

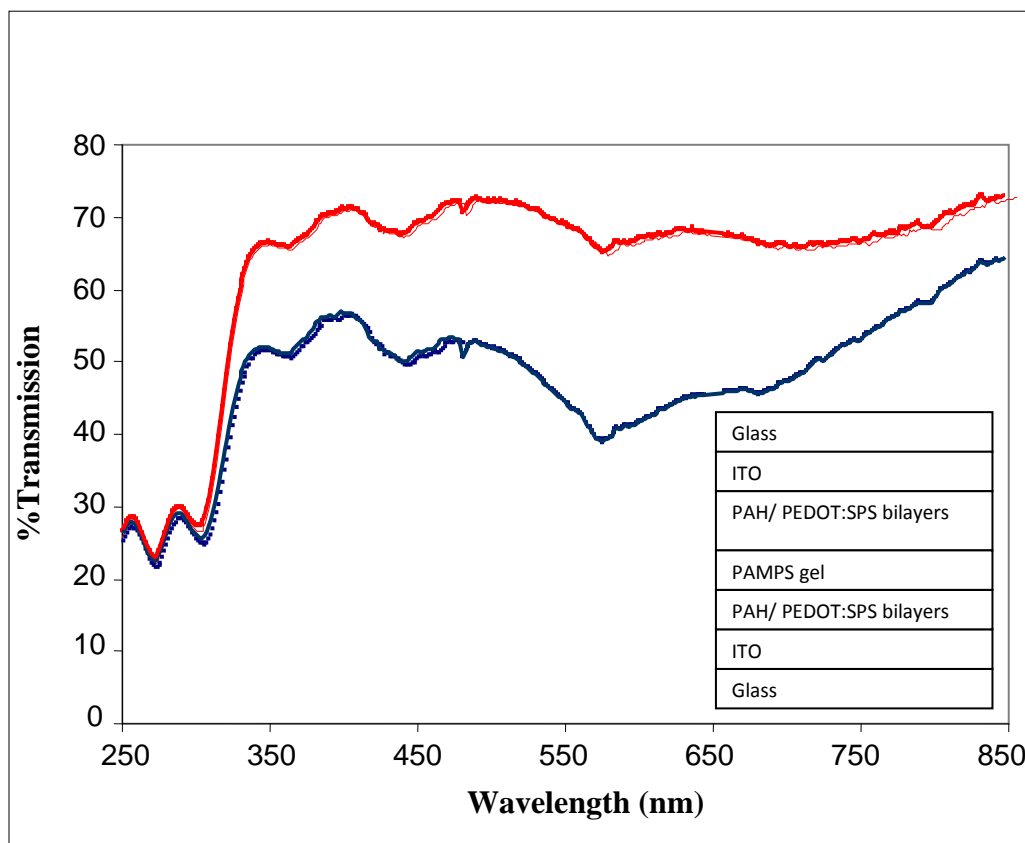


Figure 2-1. Percentage transmission vs wavelength of an electrochromic device consisting of two PAH/PEDOT 80 bilayer films with 2.0 and 0 V applied.

Symmetric PEDOT EC devices in which one of the PEDOT layers acts as a conductive electrode material have been demonstrated by Mecerreyes *et al.*¹⁵ In the present work, a

completely symmetric and reversible PEDOT EC device has been demonstrated on ITO electrodes such that, dependent upon the polarity of the applied voltage, only the PEDOT film connected to the negative terminal exhibits a color change.

2.4 Results and Discussions

The transmission spectrum of the (PAH/PEDOT:PSS)₈₀ (consisting of two 80 bilayer films) device is presented in Figure 2-1 at 0 V and with 2 V applied, as measured with a Filmetrics F20 UV-vis spectrometer. The color change is between very pale blue and dark blue. The maximum change in transmittance between 0 and 2 V is 35% at 580 nm. The temporal response of the devices was monitored with a He–Ne laser and photodiode as a square wave voltage (0–1.4 V) was applied to the electrochromic device. Figure 2-2 shows the electrochromic film response as well as the applied square wave voltage signal for a 40 bilayer (two 40 bilayer films) 1 cm² area PAH/PEDOT device. Figure 2-3 shows the fast electrochromic time response of coloration and decoloration of the 0.6 cm² (PAH/PEDOT:PSS)₄₀ device. The coloration and decoloration times (to 90% of equilibrium value) are 31 ms and 6 ms, respectively.

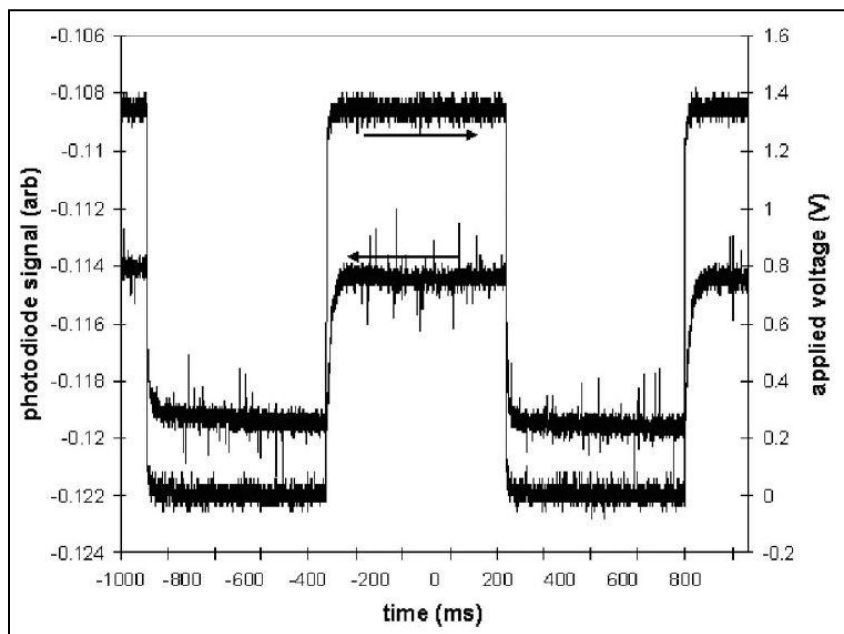


Figure 2-2. Photodiode signal vs time with square wave voltage applied for a device consisting of two 40 bilayer films with 1 cm² area.

We note that the decoloration time is shorter than the coloration time for these devices, as has been previously observed.¹ In addition, the coloration and de-coloration times of a 20 bilayer of 1 cm² device are approximately 20 and 8 ms, respectively, indicating that thinner devices switch faster, as would be expected due to the decreased transit time for the ionic motion. The contrast associated with our switching experiments at 633 nm, which is not the wavelength of maximum contrast, is approximately 8% and 5% for 40 bilayer and 20 bilayer, devices, respectively.

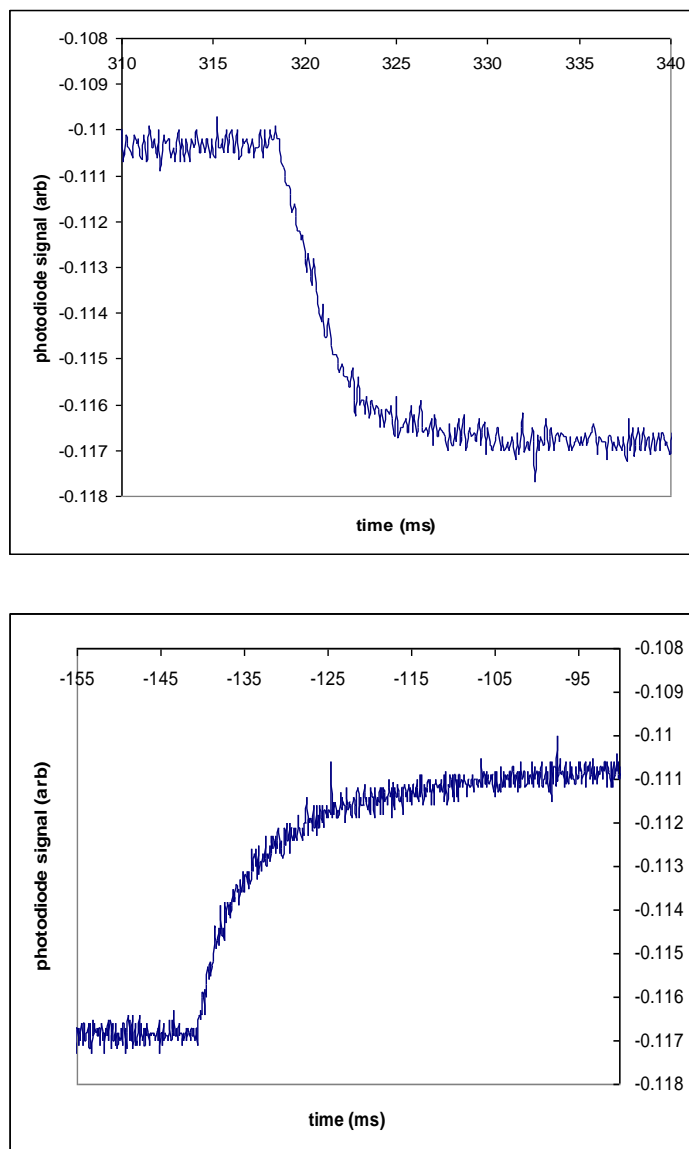


Figure 2-3. Decoloration (a) and coloration (b) of a 0.6 cm² device consisting of two 40 bilayer PAH/PEDOT films with applied voltage of 0–1.4 V.

In Figure 2-4, we show the relationship between switching speed ($t_{90\%}$) and the area of device, where $t_{90\%}$ is the time for the film to achieve 90% of its full electrochromic response. The film response time decreases linearly with the active area of the device, similar to the response of a RC circuit. Pixel areas associated with active displays are often $<0.05 \text{ cm}^2$. The relationship in Figure 2-4 suggests that switching times for 0.05 cm^2 area devices should be on the order of 3 ms for coloration and 0.6 ms for decoloration. It is anticipated that a combination of smaller area and increased polymer thickness can, thus, provide for very fast switching and significantly higher contrast than that measured here.

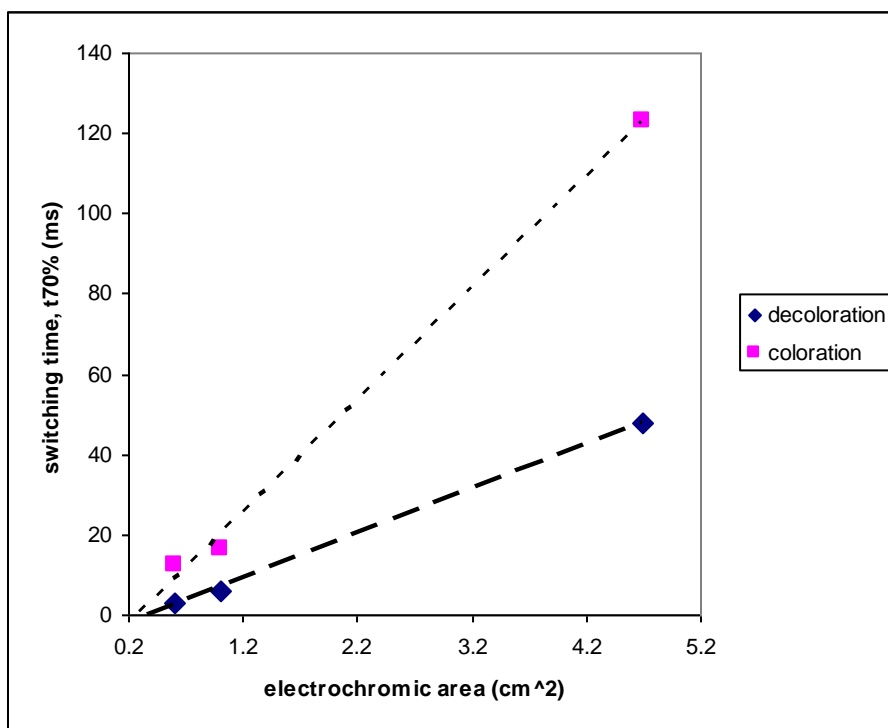


Figure 2-4. Decoloration and coloration switching times vs electrochromic device area for devices consisting of two 40 bilayer PEDOT films. Lines shown to guide the eye.

2.5 Conclusion

We have demonstrated the fast switching of an ionic self-assembled multilayer solid-state polymer electrochromic device compatible with flat-panel display rates. Devices consisting of two 80 bilayer PAH/PEDOT films display a maximum contrast of 35% at 580 nm. Devices with an active area of 0.6 cm^2 made from two 40 bilayer (400 nm thick) films show coloration and

decoloration times of 31 and 6 ms, respectively, with a linear scaling of the switching speed with the active area of the device. The fast switching is obtained through the combination of a number of factors: fabrication of thin, homogeneous films by self-assembly that have a large diffusion coefficient and short distance required for ionic motion, use of the symmetric quasi solid state geometry with a thin layer of electrolyte gel, and recognition of the dependence of the response time on device area. These results suggest that ISAM electrochromic devices are potential candidates for next-generation flat-panel displays.

2.6 References

1. D. M. DeLongchamp, M. Kastantin and P. T. Hammond, *Chemistry of Materials* 2003, **15**, 1575-1586.
2. D. M. DeLongchamp and P. T. Hammond, *Advanced Materials*, 2001, **13**, 1455-1459.
3. Z. Tang, S. T. Donohoe, J. M. Robinson, P. A. Chiarelli and H.-L. Wang, *Polymer*, 2005, **46**, 9043-9052.
4. A. L. Holt, J. M. Leger and S. A. Carter, *applied Physics Letters*, 2005, **86**, 123504-123503.
5. A. Kumar, D. M. Welsh, M. C. Morvant, F. Piroux, K. A. Abboud and J. R. Reynolds, *Chemistry of Materials* 1998, **10**, 896-902.
6. S. I. Cho, W. J. Kwon, S.-J. Choi, P. Kim, S.-A. Park, J. Kim, S. J. Son, R. Xiao, S.-H. Kim and S. B. Lee, *Advanced Materials*, 2005, **17**, 171-175.
7. G. Decher, *Science* 1997, **277**, 1232-1237.
8. P. T. Hammond, *Advanced Materials*, 2004, **16**, 1271-1293.
9. J. R. Heflin, C. Figura, D. Marciu, Y. Liu and R. O. Claus, *Applied Physics Letters*, 1999, **74**, 495-497.
10. J. R. Heflin, M. T. Guzy, P. J. Neyman, K. J. Gaskins, C. Brands, Z. Wang, H. W. Gibson, R. M. Davis and K. E. Van Cott, *Langmuir*, 2006, **22**, 5723-5727.
11. Z. Wang, J. R. Heflin, R. H. Stolen and S. Ramachandran, *Applied Physics Letters*, 2005, **86**, 223104-223103.
12. O. Onitsuka, A. C. Fou, M. Ferreira, B. R. Hsieh and M. F. Rubner, *Journal of Applied Physics*, 1996, **80**, 4067-4071.
13. H. Mattoussi, M. F. Rubner, F. Zhou, J. Kumar, S. K. Tripathy and L. Y. Chiang, *Applied Physics Letters*, 2000, **77**, 1540-1542.
14. J. K. Mwaura, M. R. Pinto, D. Witker, N. Ananthakrishnan, K. S. Schanze and J. R. Reynolds, *Langmuir* 2005, **21**, 10119-10126.
15. D. Mecerreyes, R. Marcilla, E. Ochoteco, H. Grande, J. A. Pomposo, R. Vergaz and J. M. Sánchez Pena, *Electrochimica ACTA*, 2004, **49**, 3555-3559.

Chapter 3: Single Electrochromic ECD Based on PASA LbL Thin Film

Optical Properties of an Electrochromic Device Based on a Poly (aniline 2-sulfonic) acid (PASA) Film Formed by Ionic Self-Assembled Multilayers (ISAM) Technique

Published in Journal of Undergraduate Materials Research

Authors: Montazami, R.; Jain, V.; Heflin, J.R.

3.1 Abstract

An electrochromic device (ECD) was designed and fabricated via layer by layer (LbL) assembly of poly(aniline 2-sulfonic) acid, (PASA), as the electrochromic polyanion, and poly (allylamine hydrochloride), (PAH), as the inactive polycation. Cyclic Voltammetry (CV) was employed to study the redox properties of the polymer film and to help to determine the optimal operating voltage of the device. It was determined that the PAH/PASA ECD has three redox states between -1V and $+1\text{V}$. The thin film of (PAH/PASA)₄₀ demonstrated a color change from dark green to light brown to dark gray, in $\pm 1\text{ V}$ window. The two major redox current peaks occurred at $\sim +0.3\text{ V}$ and $\sim 0\text{ V}$; another oxidation peak was observed at $\sim -0.6\text{ V}$ which had a smaller intensity. The highest transmittance contrast in the visible spectrum was approximately 30% and was observed at 690 nm.

3.2 Introduction

Electrochromic materials change color in response to an applied voltage.¹⁻² Under application of an electric field, the molecules undergo a change in their chemical structure due to the transition of electrons which result in changes in the optical density and therefore the color of the material. Under application of the electric field, the flow of electrons changes the electron wavefunctions and densities in and between molecules and surrounding electrolyte solution by reduction or oxidation processes. The conditions at which these changes occur are termed redox states.

Electrochromic devices (ECDs) consist of thin films of electrochromic materials deposited on transparent, conductive electrodes, usually glass coated with indium tin oxide (ITO).³⁻⁴ To date, some of the applications of ECDs are seven-segment displays,⁵ anti-glare mirrors,^{1, 6} and

solar-attenuated windows.⁷⁻⁸ Other possible future applications of ECDs include flat panel displays,⁹ security windows, and optical switches.¹⁰

In this work we report the electrochromic properties of a single-electrochrome ECD based on poly(aniline 2-sulfonic) acid, (PASA) which is an active electrochromic polyanion, and poly(allylamine hydrochloride), (PAH), a non-electrochromic polycation. PAH is transparent with no electrochromic attributes and it is only used for the sake of forming thin films. The layer-by-layer (LbL) assembly technique was employed to fabricate the polymer thin films, also known as ionic self-assembled multilayers (ISAMs), on the substrates. In this method oppositely charged polymers are used to buildup multiple layers of polymers on a glass substrate coated with indium tin oxide (ITO). Due to the opposite charge of neighboring layers, they are bound together to form the polymer thin film.¹¹⁻¹³ Through control over the molecular weight,¹⁴ pH,¹⁵⁻¹⁷ ion type,¹⁴ ion concentration¹⁸ and ionic strength¹⁹ of the ionic species, the LbL assembly technique makes it possible to have nanometer control on the thickness of the monolayers and the thin film as a whole, as well as control over morphology of the thin film. Usually the films formed via the LbL assembly technique are very homogenous, which is especially important for optical devices. LbL assembled films are very stable and robust due to the strong ionic interactions between cationic and anionic layers. Figure 3-1 shows a schematic of the formation of bilayers in the LbL assembly technique.

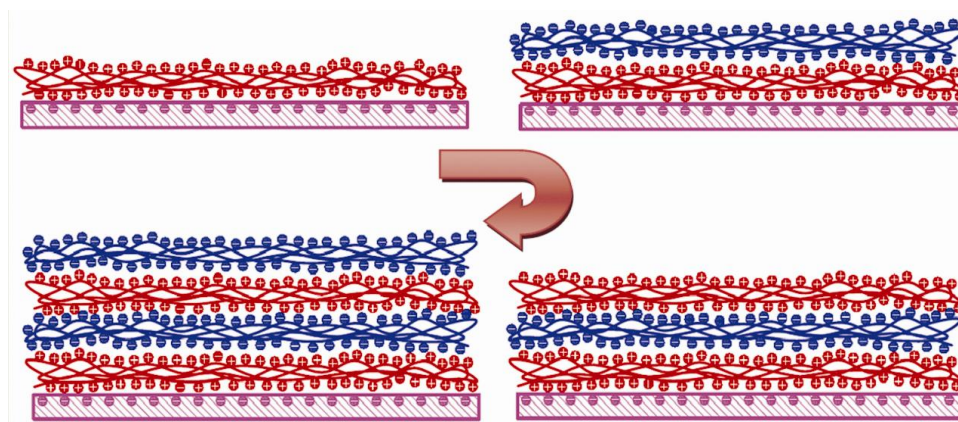


Figure 3-1. LbL assembly technique. Layers of oppositely charged polymers are used to construct the thin polymer film.

Devices consisting of two electrochromic polymers are termed dual-electrochromic ECDs; such devices are expected to have more redox states compared to single-electrochromic ECDs. Details of such devices can be found in several publications,²⁰⁻²¹ but this work focuses on single-electrochromic ECDs.

3.3 Materials and Methods

3.3.1 Substrate

A 25 mm x 75 mm x 0.7 mm unpolished float glass, SiO₂ passivated with ITO coating on one surface ($R_s = 8 - 12 \ \Omega/\text{sq}$) (Delta Technologies, USA) was used as the transparent conducting substrate. The uncoated side of the substrate and about 20 mm of the ITO coated side of the substrate were covered by electrical tape to prevent deposition of the polymer thin film on these surfaces. The substrate was then cleaned in piranha bath, washed with deionized (DI) water, and dried with nitrogen. The substrate was then exposed to NaOH solution to increase the hydrophilicity of its surface.

3.3.2 Solutions

All chemicals were reagent grade and were used as received. DI water was used throughout the entire solution preparation process. All chemicals were commercially available (Sigma-Aldrich, USA). 2 mM PASA solution (pH 3) was used as polyanion and 10 mM PAH (pH 9) was used as polycation. Both solutions are water based and freshly prepared prior to use.

3.3.3 Film Deposition

The LbL technique was used to deposit a thin film of PAH/PASA on the substrate. Deposition was done at room temperature, using an automatic dipping machine. To form the first bilayer the sample was: 1) exposed to PAH by spinning it in PAH bath for 4 minutes; 2) then washed in three steps, 45 seconds each, with DI water to remove any loosely bound PAH molecules. After forming the first monolayer, the sample was; 3) exposed to PASA by spinning it in PASA solution for 5 minutes and then; 4) washed with DI water in three steps, 45 seconds each, to remove any loosely bound PASA molecules. These four steps were to form one bilayer, consisting of one polycation and one polyanion layer. This process was repeated 40 times to form a thin PAH/PASA film of 40 bilayers. This process can be repeated any desired number of

times and can be used to control the thickness of the LbL assembled thin film. Other factors such as dipping duration and the pH of the solutions can also affect the thickness and quality of the thin films. The electrical tape were then removed.

Scanning electron microscopy (SEM) was used to investigate the thickness of the LbL assembled thin film. The thickness of each bilayer is estimated to be 30 – 35 nm. The SEM of the cross section of the film, shown in Figure 3-2, suggests homogeneity in deposition.

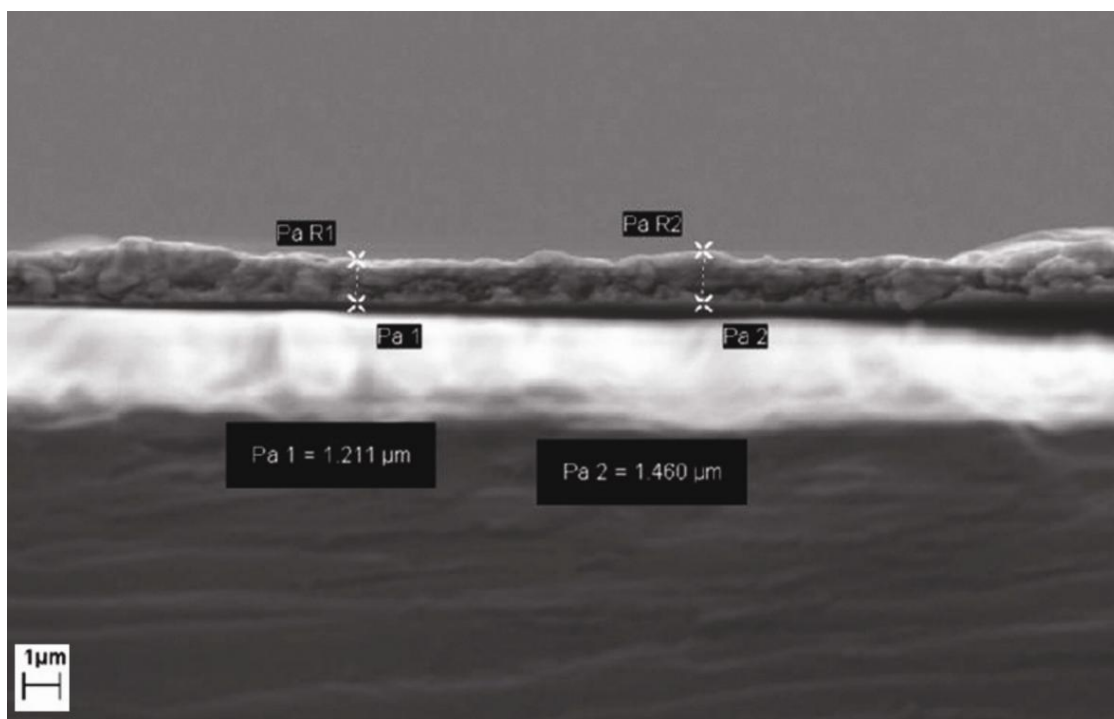


Figure 3-2. SEM image of 40 bilayers of PAH / PASA on ITO

3.4 Results and Discussions

3.4.1 Cyclic Voltammetry

Cyclic voltammetry (CV) was used to characterize the electrochemical properties of the (PAH/PASA)₄₀ film in 0.1 M NaClO₄ aqueous electrolyte solution. A standard calomel electrode (SCE) was used as the reference electrode and a platinum flag as the counter electrode. The thin film was scanned between ± 1 V at different scan rates to determine the redox potentials and reaction type. As shown in Figure 3-3, at 25 mV/s scan rate the major reduction peak occurred at approximately 0.3 V and the corresponding oxidation peak appeared at approximately 0 V. A second, smaller oxidation peak was observed at approximately -0.6 V. As the scan rate was

increased to 50 mV/s and 100 mV/s the current peaks shifted outward which indicates the separation between reaction zone and the surface of the electrode which is due to the thickness of the thin film.

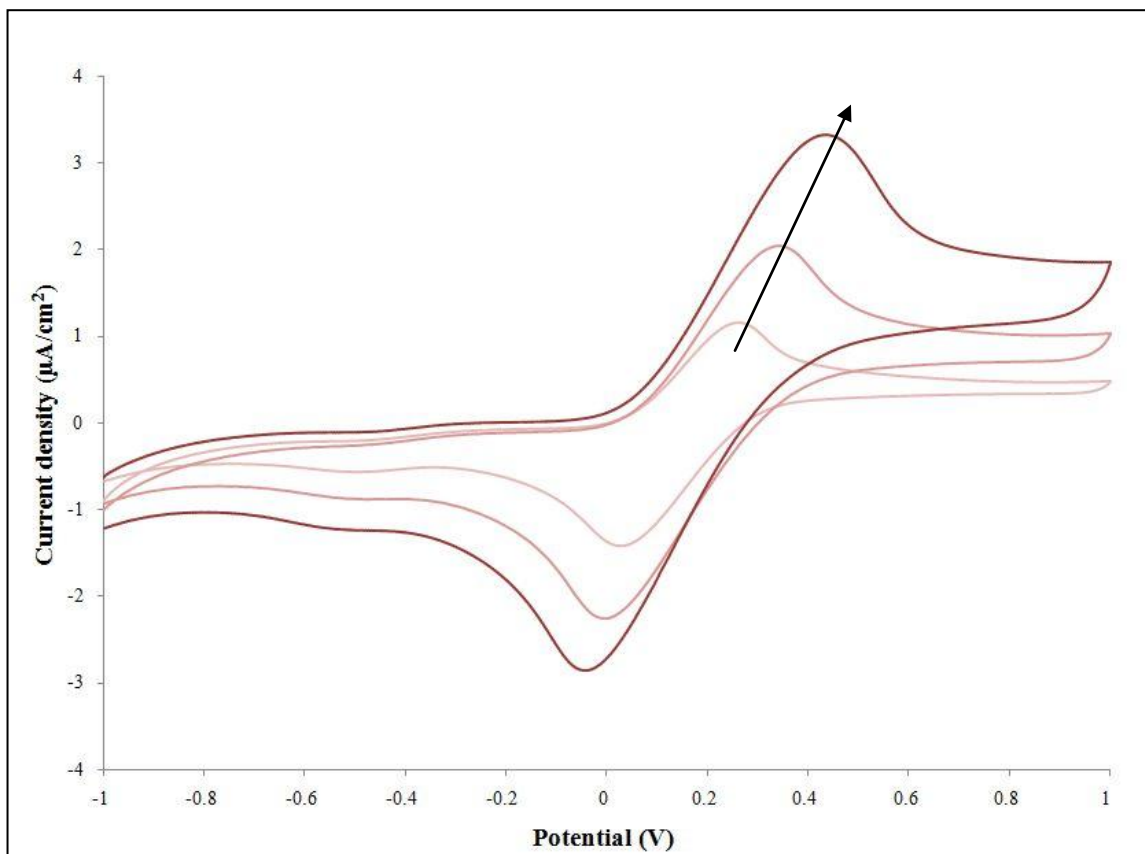


Figure 3-3. Cyclic Voltammetry of $(\text{PAH/PASA})_{40}$ at 25, 50 and 100 mV/s scan rates. A reduction peak was observed at $\sim +0.3$ V and oxidation peaks at ~ 0 V and ~ -0.6 V. The arrow indicates increasing scan rate.

3.4.2 Color Change

The $(\text{PAH/PASA})_{40}$ ECD was tested in a electrochemical cuvette to confirm its color change. The device was immersed in 0.1 M NaClO_4 electrolyte while a voltage was applied across the device and a copper counter electrode. The device exhibited color change at $\sim +0.3$ V and ~ -0.6 V. Figure 3-4 shows photos of the device at different redox states.

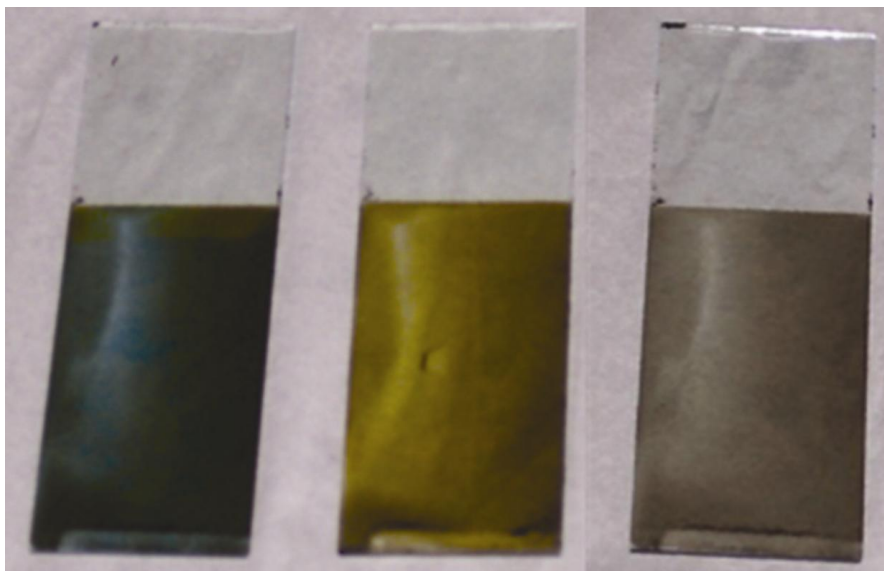


Figure 3-4. Color of (PAH/PASA)₄₀ at different redox states. From left to right, oxidized, neutral and reduced.

3.4.3 Spectroelectrochemistry:

The electrochromic characteristics of PASA were investigated by spectroelectrochemistry. In this method, a collimated beam of light with varying wavelength from 400 nm to 1100 nm was shone on the device and the transmitted light was collected at the other end of the apparatus for measurement of the transmitted and absorbed wavelengths.

The ITO electrode coated with the (PAH/PASA)₄₀ film was tested in a cuvette electrochemical cell filled with 0.1M NaClO₄. The intensity of transmitted visible spectrum through the thin film was measured at neutral, oxidation and reduction potentials, 0, -0.8 and +0.8 Volts respectively. As shown in Figure 3-5, the highest contrast in the visible spectrum was about 30% at approximately 690 nm.

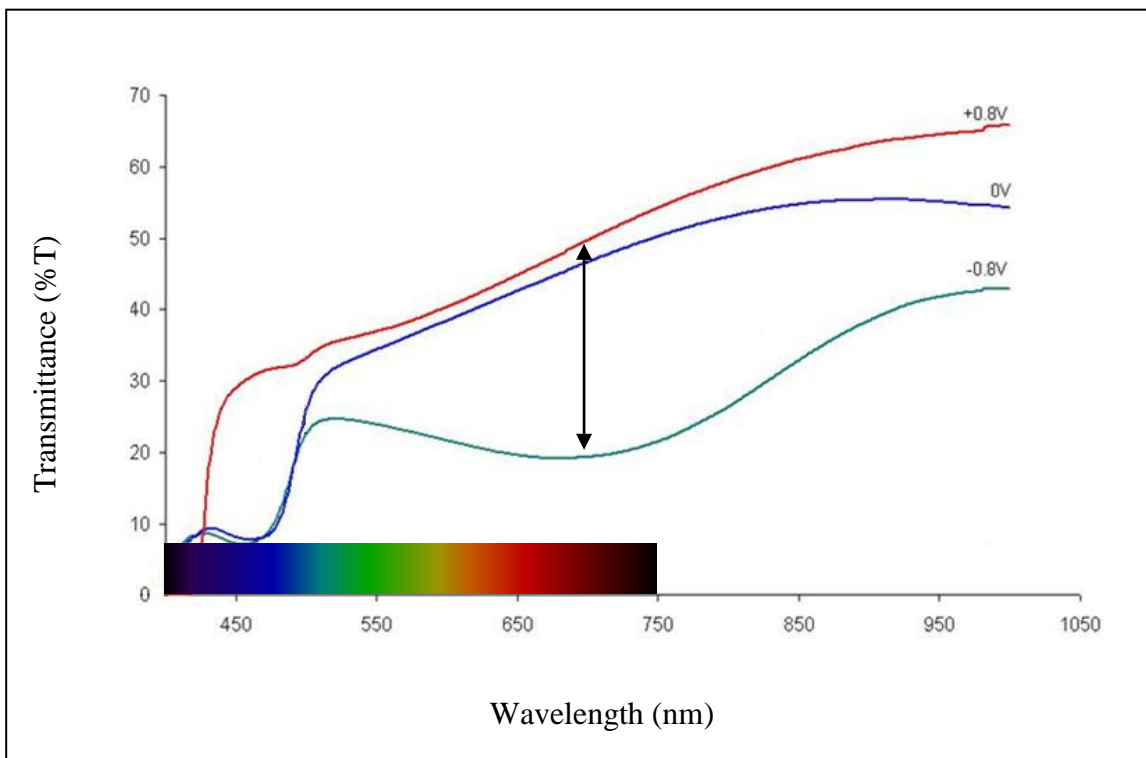


Figure 3-5. Transmittance of $(\text{PAH/PASA})_{40}$ at neutral and redox states. The highest contrast is about 30% and was observed at ~ 690 nm.

3.5 Conclusion

The electrochromic properties of a thin film system based on PASA was investigated in this paper. PASA was found to have interesting and promising electrochemical properties. $(\text{PAH/PASA})_{40}$ exhibited three redox states in the -1.0 V to $+1.0$ V range. The color change remains after removing the voltage, which suggests that the ECD has long-term memory. According to the CV data, the polymer film reduces at $+0.3$ V and oxidizes at ~ 0 V and -0.6 V. The device changes color at both oxidation and reduction states, which agrees with the results from the CV. The device showed about 30% contrast between redox states at 690 nm.

3.6 References

1. Mortimer, R. J., Electrochromic Materials *Chemical Society Reviews* **1997**, 26, 147-156.
2. Somani, P. R.; Radhakrishnan, S., Electrochromic materials and devices: present and future. *Materials Chemistry and Physics* **2003**, 77, (1), 117-133.
3. Granqvist, C. G.; Avendaño, E.; Azens, A., Electrochromic coatings and devices: survey of some recent advances. *Thin Solid Films* **2003**, 442, (1-2), 201-211.
4. Granqvist, C., Electrochromic devices. *Journal of the European Ceramic Society* **2005**, 25, (12), 2907-2912.
5. Kim, E.; Jung, S., Layer-by-layer assembled electrochromic films for all-solid-state electrochromic devices. *Chemistry of Materials* **2005**, 17, (25), 6381-6387.
6. Kobayashi, T.; Fujita, K.; Muto, J., Characteristics of electrochromic magnesium phthalocyanine films for repeated oxidation-reduction cycling. *Journal of Materials Science Letters* **1996**, 15, (14), 1276-1278.
7. Cui, M.-H.; Guo, J.-S.; Xie, H.-Q.; Wu, Z.-H.; Qiu, S.-C., All-solid-state complementary electrochromic windows based on the oxymethylene-linked polyoxyethylene complexed with LiClO. *JOURNAL OF APPLIED POLYMER SCIENCE* **1997**, 65, (9), 1739-1744.
8. Rauh, R. D., Electrochromic windows: an overview. *ELECTROCHIMICA ACTA* **1999**, 44, (18), 3165-3176.
9. Jain, V.; Yochum, H.; Montazami, R.; Heflin, J., Millisecond switching in solid state electrochromic polymer devices fabricated from ionic self-assembled multilayers. *Applied Physics Letters* **2008**, 92, (3), -.
10. Armitage, R.; Rubin, M.; Richardson, T.; O'Brien, N.; Chen, Y., Solid-state gadolinium--magnesium hydride optical switch. *APPLIED PHYSICS LETTERS* **1999**, 75, (13), 1863-1865.
11. Lutkenhaus, J. L.; Hammond, P. T., Electrochemically enabled polyelectrolyte multilayer devices: from fuel cells to sensors. *Soft Matter* **2007**, 3, (7), 804-816.
12. Iller, R. K., Multilayers of colloidal particles. *Journal of Colloid and Interface Science* **1966**, 21, 569-594.
13. Decher, G. H., J.D., Buildup of ultrathin multilayer films by a self-assembly process 1. Consecutive adsorption of anionic and cationic bipolar amphiphiles on charged surfaces. *Macromol. Chem., Macromol. Symp* **1991**, 46, 231.
14. Clark, S. L.; Montague, M.; Hammond, P. T., Selective deposition in multilayer assembly: SAMs as molecular templates. *Supramolecular Science* **1997**, 4, (1-2), 141-146.
15. Yoo, D.; Shiratori, S.; Rubner, M., Controlling bilayer composition and surface wettability of sequentially adsorbed multilayers of weak polyelectrolytes. *MACROMOLECULES* **1998**, 31, (13), 4309-4318.
16. Shiratori, S. S.; Rubner, M. F., pH-Dependent Thickness Behavior of Sequentially Adsorbed Layers of Weak Polyelectrolytes. *MACROMOLECULES* **2000**, 33, (11), 4213-4219.
17. Dubas, S.; Schlenoff, J., Polyelectrolyte multilayers containing a weak polyacid: construction and deconstruction. *MACROMOLECULES* **2001**, 34, (11), 3736-3740.
18. Bungenberg de Jong, H., Crystallisation-coacervation-flocculation. *Colloid Science* **1949**, 2, 232-255.

19. Clark, S.; Montague, M.; Hammond, P., Templating of Layer-by-Layer Thin Films: Use of Surface Functionality to Direct Polyion Deposition. *POLYMERIC MATERIALS SCIENCE AND ENGINEERING-WASHINGTON-* **1997**, 77, 620-621.
20. DeLongchamp, D. M.; Kastantin, M.; Hammond, P. T., High-contrast electrochromism from layer-by-layer polymer films. *Chemistry of Materials* **2003**, 15, (8), 1575-1586.
21. DeLongchamp, D. M.; Hammond, P. T., Multiple-color electrochromism from layer-by-layer-assembled polyaniline/Prussian blue nanocomposite thin films. *Chemistry of Materials* **2004**, 16, (23), 4799-4805.

Chapter 4: Dual Electrochrome ECD Based on PANI and PASA Thin Films

High Contrast Asymmetric Solid State Electrochromic Devices Based on Layer-by-Layer Deposition of Polyaniline and Poly(aniline 2-sulfonic) acid

Submitted to Physical Chemistry Chemical Physics

Authors: Montazami, R.; Jain, V.; Heflin, J.R.

4.1 Abstract

Layer-by-layer (LbL) self-assembly was employed for alternating deposition of two electrochromic polymers to fabricate a single film composite. We report a wide spectral range, high contrast asymmetric solid state electrochromic device, fabricated by LbL assembly of the polycation polyaniline (emeraldine base) (PANI) and the polyanion poly(aniline 2-sulfonic) acid, (PASA). Detailed spectral investigation of the dual electrochrome thin film confirms that both electrochromic polymers contribute to the electrochromic and electrochemical characteristics of the composite. Under the application of +/- 2.3 V potential the system exhibited an average contrast of 50% across the full visible spectrum. The dual electrochrome system was compared to single electrochrome systems, and it was observed that PANI predominantly affects the electrochromic optical spectra of the composite, whereas PASA increases the switching speed. Electrochemical studies of a device containing 40 bilayers of PANI/PASA showed reversible electrochemical properties.

4.2 Introduction

Due to variations in redox states, electrochromic (EC) devices exhibit changes in their optical transmittance. The variations in the redox states are caused by controlling the potential difference between the electrodes of the device. EC devices based on a variety of inorganic compounds,¹⁻³ polymers⁴⁻¹⁰ and phthalocyanines¹¹⁻¹³ have been previously studied. In this work we present EC devices based on a pair of electrochromic polymers.

Thin-films can be created through several methods including chemical vapor deposition, electron beam deposition, Langmuir-Blodgett technique, and layer-by-layer (LbL) self-assembly technique. In the case of electronically functional thin-films, thinner films are generally preferred

because of the shorter electron and ion transport path length.

The LbL assembly technique provides nanoscale thickness control for fabrication of thin films and is one of the most popular techniques for fabricating thin polymer films. The LbL technique consists of repeated cycles of alternating adsorption of cationic and anionic materials from aqueous solutions onto the substrate.¹⁴⁻¹⁵ Varying the number of cycles results in a different number of bilayers and is one way to control the thickness of the thin film from the nanometer to micron scale. Other factors, such as pH and ionic strength of the electrolyte solutions, can also be used to tune the thickness of the material adsorbed into individual layers. Because of its low cost, high precision, and ease of production, the LbL technique is one of the easiest and simplest methods to implement.¹⁶⁻¹⁸ Another significant advantage of using the LbL technique is that any charged species can be incorporated into a thin film.

Polyaniline (PANI) is an electronically conductive and electrochromically active polymer. The optical and structural properties,¹⁹ switching speed,²⁰ and optical properties of PANI in solid state EC devices²¹ have been previously studied. Several forms of PANI exist. One is the emeraldine salt (ES) which is conductive and green in color, and another is the emeraldine base (EB) which is blue in color and an insulator.²² PANI (ES) is not stable in the presence of moisture and converts into PANI (EB), which is the more oxidized form. PANI-based electrochromic devices have been previously studied by several groups. Hu *et al.*²² studied the electrochromic properties of PANI along with poly(2-acrylamido 2-methylpropane sulfonic acid) (PAMPS) and reported maximum transmittance contrast of approximately 40% at a wavelength of approximately 580 nm and a switching time of 10 seconds under application of +/- 2.0 V. In a similar study, Hechavarria *et al.*²³ achieved maximum transmittance contrast of approximately 45% at approximately the same wavelength. DeLongchamp *et al.*²⁴ performed a more in-depth study of PANI based EC devices fabricated through the layer-by-layer technique. They reported maximum transmittance contrast of 51.7% at a wavelength of 748 nm for an EC device consisting of 20 bilayers of PANI and PAMPS and a contrast of 24% for a device consisting of 20 bilayers of PANI and PEDOT. The device exhibited fast switching speeds of 0.37 s and 1.22 s for bleaching and coloration, respectively.

In this study, we used PANI (EB) as the polycation and poly(aniline 2-sulfonic) acid (PASA) as the polyanion. PASA is also an electronically conductive and electrochromically active polymer²⁵ that has been characterized by conductivity, elemental, and spectroscopic

analysis.²⁶⁻²⁸ Sarkar *et al.*²⁵ studied the electrochromic properties of sulfonated polyaniline versus the physical properties of PASA LbL films and reported that the absorbance of the device increases linearly with the number of bilayers. By combining cationic and anionic polyaniline forms together into a single LbL film, we anticipated changes in electrochromic and electrochemical properties of the film compared to the films constructed of either PANI or PASA paired with a non-electrochromic polymer. In this work, we study the electrochromic and electrochemical properties of PANI/PASA solid state dual electrochrome EC devices with varying thickness and voltage. The thickness of the thin film can be easily controlled through the number of layer pairs, referred to as bilayers.

4.3 Materials and Methods

All solutions were freshly prepared prior to the LbL self-assembly process and were used within one week of the preparation date. All the chemicals used are commercially available (Sigma-Aldrich). Deionized (DI) water was used for the immersion and rinsing solutions. Solutions were prepared at ambient conditions.

Since polyaniline is not soluble in water, a different technique, inspired by Cheung *et al.*²⁹, was used to prepare the solution. 1) Polyaniline was added to dimethylacetamide (DMAc) at ratio of 20 mg/ml; 2) the solution was then stirred overnight and 3) sonicated at 40°C for two hours. 4) The solution was slowly added to DI water nine times its volume with pH 3.25. 5) The pH of the solution was immediately reduced to 3.0. 6) The solution was then stirred for three more hours and then 7) filtered using filter paper with retention of 11 µm. The solution was kept at ambient temperature and used within seven days.

In order to make 300 ml of 10 mM PASA solution, 500 mg of poly(aniline 2-sulfonic) acid was mixed into 300 ml of DI water and was left to stir for about 5 hours. The pH of the solution was 2.9 and was increased to 4.2. The solution was kept at ambient temperature and used within seven days.

All devices were made using 25x75x0.7 mm³ unpolished float glass, with passivated SiO₂ and indium-tin oxide coating on one side with sheet resistance R_s of 8 to 12 Ω/square purchased from Delta Technologies Ltd. Each slide was soaked in 1 M sodium hydroxide solution for 30 minutes to make a more hydrophilic surface. The non-ITO side of each substrate was covered with electrical tape to prevent adsorption of the LbL film on that side.

An automated dipping robot (Nanostrata 6) was used to deposit the LbL films on the ITO

slide. PANI and poly(allylamine hydrochloride) (PAH) were used as polycations and PASA and poly (2-acrylamido 2-methylpropane sulfonic acid) (PAMPS) as polyanions. The immersion time for each layer of polymer was set to six minutes, followed by three consecutive washings of 45 seconds each. Thin films with different numbers of bilayers were fabricated. The thickness of films of different number of bilayers was measured by SEM of the cross-section of the thin films.

Asymmetric devices were fabricated using the ITO-coated slide with LbL film as the primary electrode and an ITO-coated slide without LbL film as the counter electrode. A few drops of PAMPS conductive gel was used to bind the two electrodes together.

4.4 Results and Discussions

4.4.1 Thickness

Films with different numbers of bilayers were made in order to examine the contrast of the film with respect to the number of bilayers. As shown in Figure 4-1, the thickness of PANI/PASA films followed an exponential behavior. While LbL films generally exhibit linear growth with the number of bilayers, exponential growth has also been observed in several cases.³⁰⁻³² The mechanism for exponential growth is not yet fully understood. The change in transmittance between the oxidized and reduced states of each sample, under application of +/- 2.3 V, is shown in Figure 4-2. The contrast of the devices is increased with the number of bilayers up to 40 bilayers. The contrast of the 50 bilayers device essentially overlaps that of 40 bilayers, and the contrast of the 60 bilayers device is slightly higher over most of the visible spectrum.

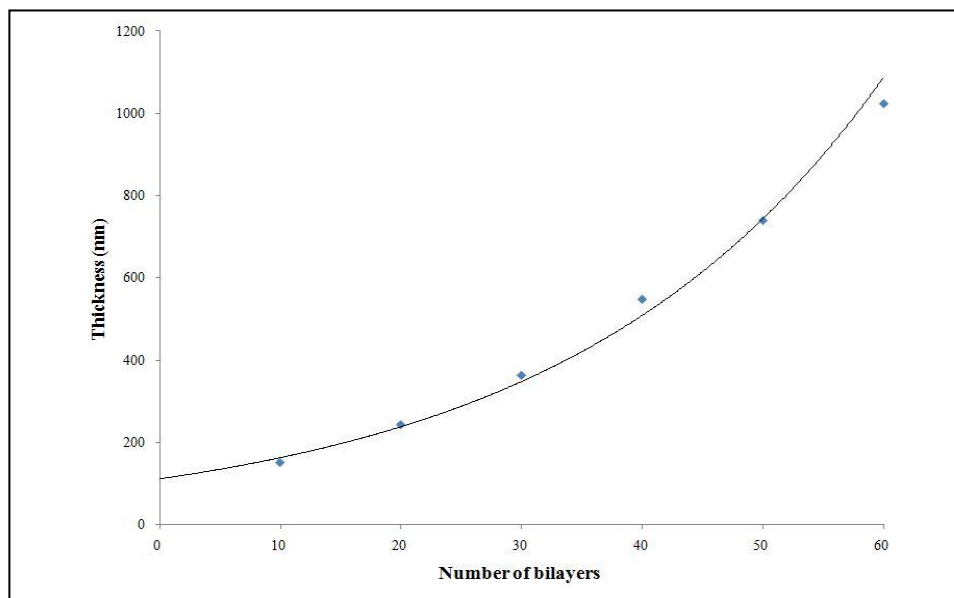


Figure 4-1. Film thickness of PANI/PASA LbL films versus number of bilayers. The curve is an exponential fit to the data.

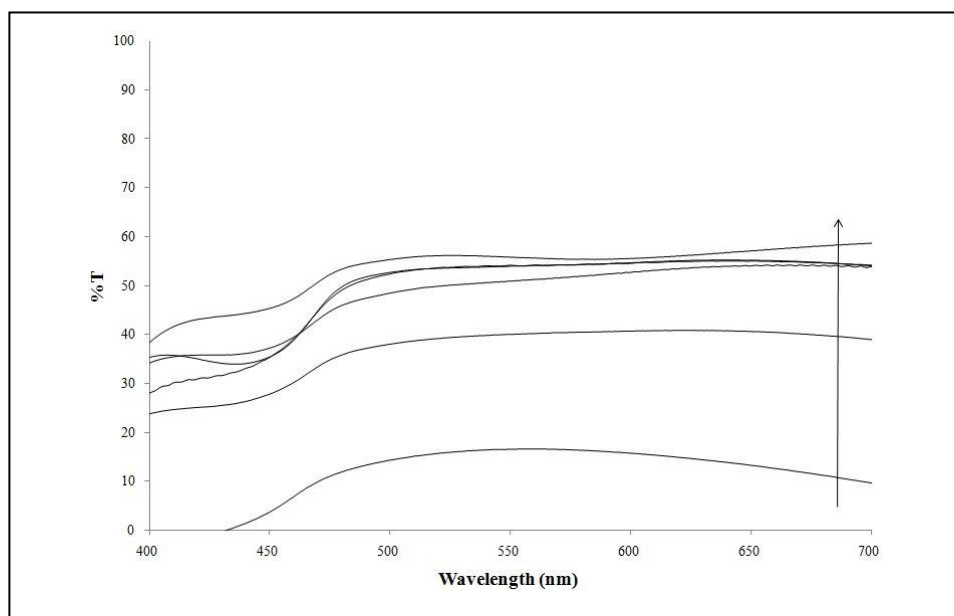


Figure 4-2. The change in transmittance between +2.3 V and -2.3 V of PANI/PASA devices with different numbers of bilayers for 10 to 60 bilayers with 10 bilayers intervals. The arrow indicates increasing number of bilayers.

4.4.2 Cyclic Voltammetry

Cyclic voltammetry (CV) was used to identify redox potential ranges and clarify general electrochemical behavior. The scanning range was set between -1.0 V and +1.0 V to cover the lowest redox potentials of both PANI and PASA. All the CV data were taken on samples of LbL films deposited onto ITO-coated float glass in a supporting 0.1 M LiClO₄ aqueous electrolyte solution. In order to better understand ion accessibility of the polymers, CV was taken at varying scan rates. In addition, to identify the contributions of PANI and PASA to the composite device, CV scans of single electrochrome films were taken. Thus, films were made of PANI/PAMPS and PAH/PASA, where PAH and PAMPS are electrochemically inactive over the scanned potential range. CV scans for (PAH/PASA)₄₀ and (PANI/PAMPS)₄₀ are shown in Figures 4-3 and 4-4, respectively, where the subscripts denote the number of bilayers of the LbL films.

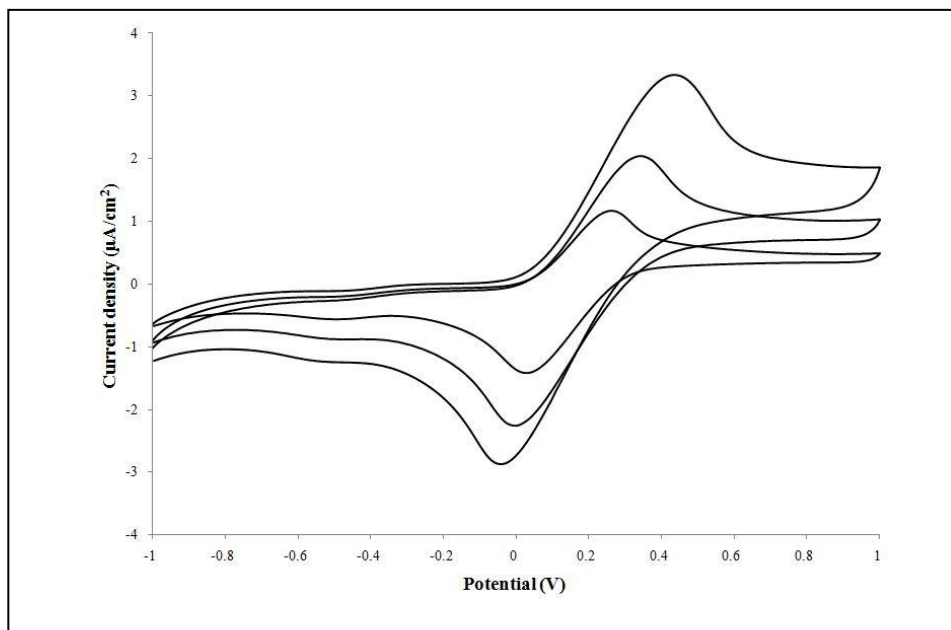


Figure 4-3. Cyclic voltammograms of (PAH/PASA)₄₀ taken at 25, 50, and 100 mV/s scan rates.

The increasing total area under the curve corresponds to increasing scan rate.

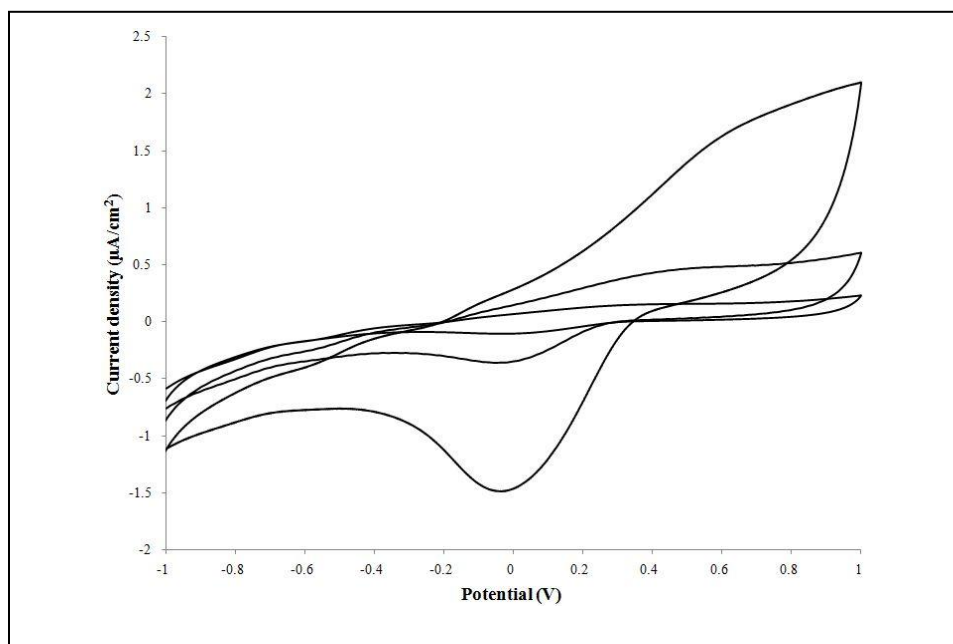


Figure 4-4. Cyclic voltammograms of $(\text{PANI/PAMPS})_{40}$ taken at 25, 50, and 100 mV/s scan rates. The increasing total area under the curve corresponds to increasing scan rate.

In the CV of the $(\text{PAH/PASA})_{40}$ sample, PASA shows two sharp redox waves and one weaker peak. The first sharp redox wave is an oxidative peak in the vicinity of 0.3-0.5 V. The position of the peak moves toward the right (positive potential) for higher scan rates, and the peak height also increases as the scan rate increases. The second sharp wave, indicating reduction of the oxidized species, appears as the potential decreases from 0.3 V. A weak reductive peak can be seen at -0.5 V, and there is the suggestion of another peak, which starts at -0.9 V and is out of the scan range.

The CV of $(\text{PANI/PAMPS})_{40}$, as shown in Figure 4-4, consists of broad redox waves. The first wave, indicating oxidation, starts at approximately -0.2 V and elevates as the potential goes up to +1.0 V, but the peak is outside of the scan window. The slope of the wave and the peak height both increase with the scan rate. The peak of the reduction wave is centered at 0.0 V and follows the same behavior as the oxidation peak.

The CV of $(\text{PANI/PASA})_{40}$, as shown in Figure 4-5, confirms that both polymers contribute to the electrochromic switching of the dual electrochrome system. At lower scan rates, the redox behavior of the dual electrochrome film is very similar to that of PANI. However, at higher scan

rate the redox behavior is more indicative of PASA. The first oxidation peak at higher scan rate clearly shows the effect of PASA.

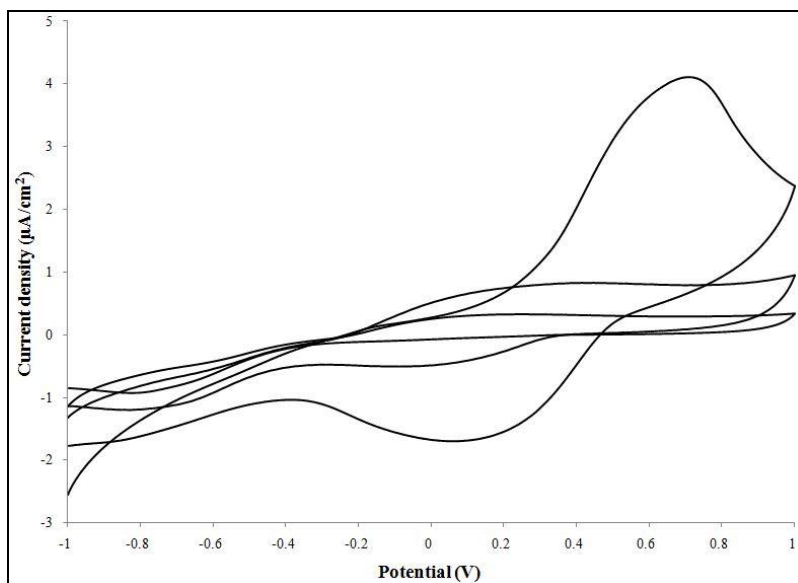


Figure 4-5. Cyclic voltammogram of (PANI/PASA)₄₀ taken at 25, 50, and 100 mV/s scan rates. The increasing total area under the curve corresponds to increasing scan rate. At higher scan rate the contribution of PASA is more obvious.

4.4.3 Contrast

Asymmetric solid state EC devices were used to investigate the optical properties in the visible spectrum at different potentials. The transmittance curves of a (PANI/PASA)₄₀ EC device shown in Figure 4-6 have significant changes in transmittance beyond +/- 1.5 V.

In Figure 4-7 we show the spectra of the (PANI/PASA)₄₀ EC device at +/- 2.3 V and 0 V potential along with the contrast plot. At positive potential the film is colored (dark blue), this coloration is in response to the oxidation of the composite. Upon application of negative potential, the composite undergoes reduction resulting in a decoloration of the film (pale yellow). One of the most significant properties of the PANI/PASA composite is the large and relatively flat change in transmittance over the entire visible spectrum. The average contrast between the colored and bleached states of the composite at +/- 2.3 V over the visible spectrum is 49.7%. The average contrast between 500-700 nm is 54.4%.

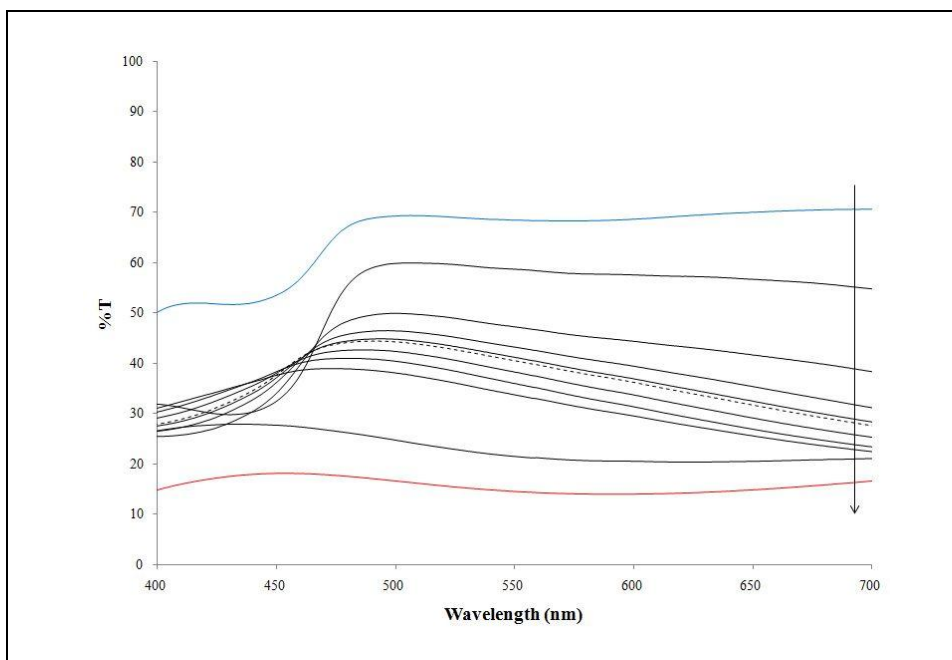


Figure 4-6. Spectra of (PANI/PASA)₄₀ asymmetric EC device taken from -2.5 V to +2.5 V at 0.5 V intervals. Dashed line indicates 0 V data, and the arrow indicates increasing potential.

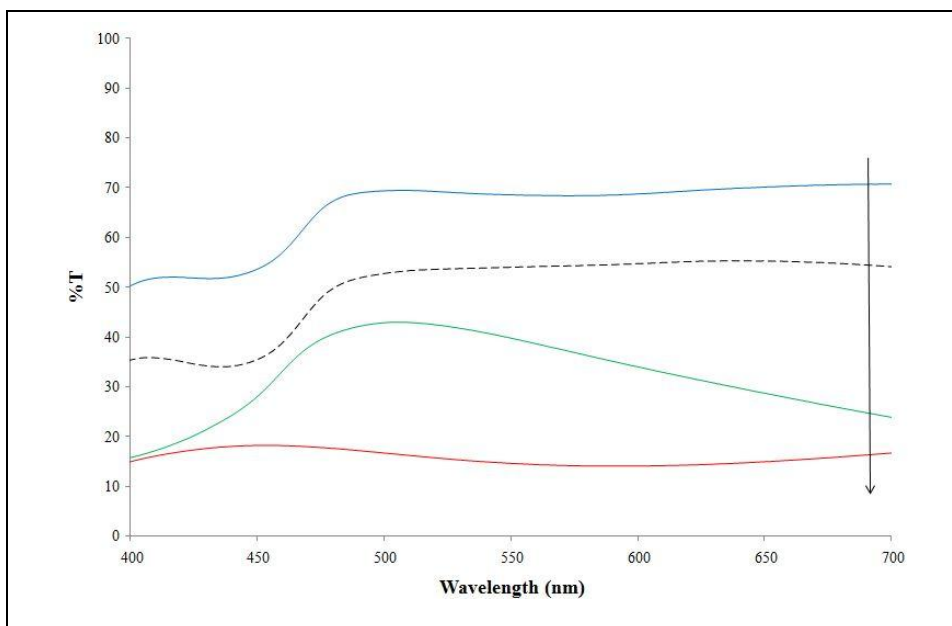


Figure 4-7. Spectra of (PANI/PASA)₄₀ asymmetric EC device taken at -2.3, 0, and +2.3 V. The dashed line indicates the change in transmittance between -2.3 V spectra and +2.3 V spectra. Arrow indicates increasing potential.

In order to determine the relative contributions of PANI and PASA to the composite device, we also fabricated EC devices in which PANI and PASA were each paired with the electrochromically inactive polyelectrolytes PAMPS and PAH, respectively. Comparison of the spectra of (PANI/PASA)₄₀ with that of (PAH/PASA)₄₀ and (PANI/PAMPS)₄₀ (shown in Figures 4-8 and 4-9, respectively) suggests that the transmittance of the PANI/PASA composite is largely influenced by PANI. While PASA has little effect on the shape of the (PANI/PASA)₄₀ spectra, the (PANI/PASA)₄₀ spectra are shifted to 10-20% higher transmittance values than the (PANI/PAMPS)₄₀ spectra. More importantly, the incorporation of PASA results in faster electrochromic switching, as shown below.

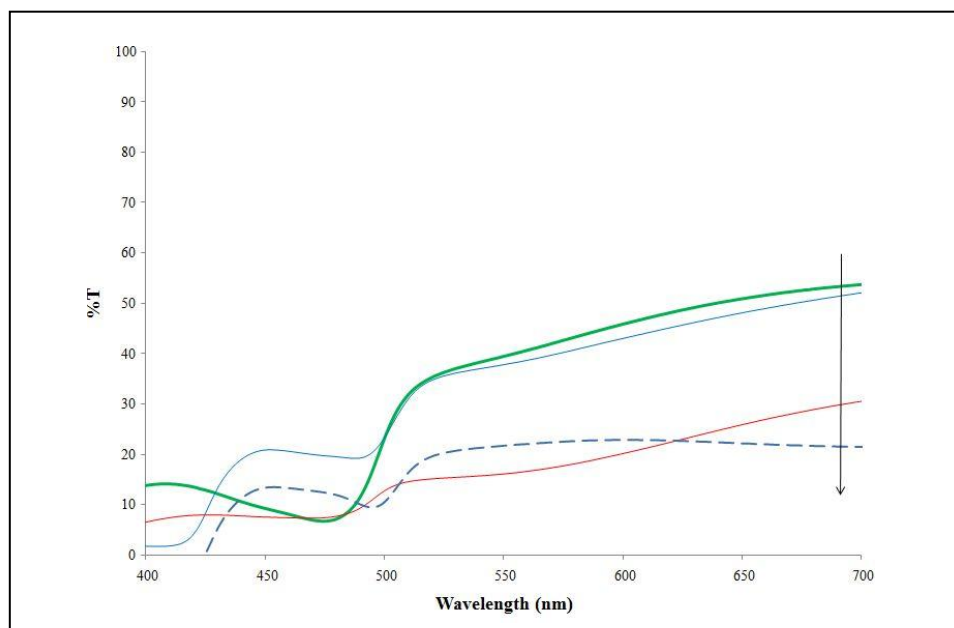


Figure 4-8. Spectra of (PAH/PASA)₄₀ asymmetric EC device taken at -2.3, 0, and +2.3 V. The bold solid line indicates the 0 V spectrum, and the dashed line indicates the change in transmittance between -2.3 V spectra and +2.3 V spectra. The arrow indicates increasing potential.

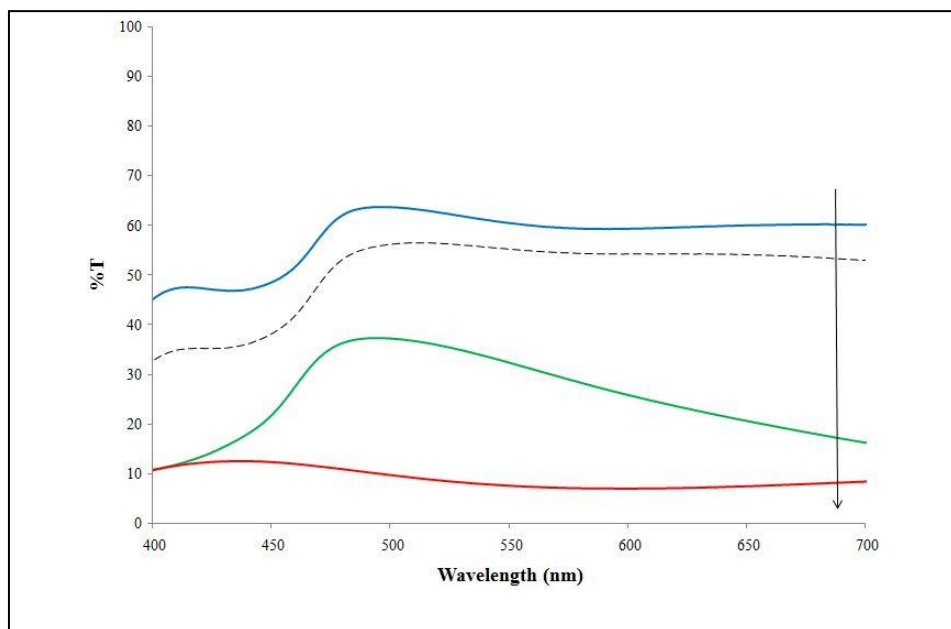


Figure 4-9. Spectra of (PANI/PAMPS)₄₀ asymmetric EC device taken at -2.3, 0, and +2.3 V. The dashed line indicates the change in transmittance between -2.3 V spectra and +2.3 V spectra. Arrow indicates increasing potential.

4.4.4 Switching Speed

The switching speeds of (PANI/PAMPS)₄₀ and (PANI/PASA)₄₀ devices were monitored over time with a He-Ne laser ($\lambda = 633 \text{ nm}$). A +/- 2.3 V square wave was applied at 0.25 Hz. As shown in Figures 4-10 and 4-11, (PANI/PASA)₄₀ showed faster electrochromic switching than (PANI/PAMPS)₄₀, as indicated by the transmittance nearly reaching its asymptotic value over the switching period for both coloration and decoloration. As a result, the PANI/PASA device also achieved a higher change in transmittance in the given period. The PANI/PASA sample reached a change in transmittance of 39.6% at 633 nm while the PANI/PAMPS sample reached a change in transmittance of 23.6%. Although the PANI/PASA device exhibits a faster coloration, neither of the devices achieves 75% of the full coloration state within the switching period of 2 seconds. For decoloration, PANI/PAMPS exhibited a similar curve to its coloration process with

reversed slope while the PANI/PASA device reached 75% of full decoloration in approximately 700 ms.

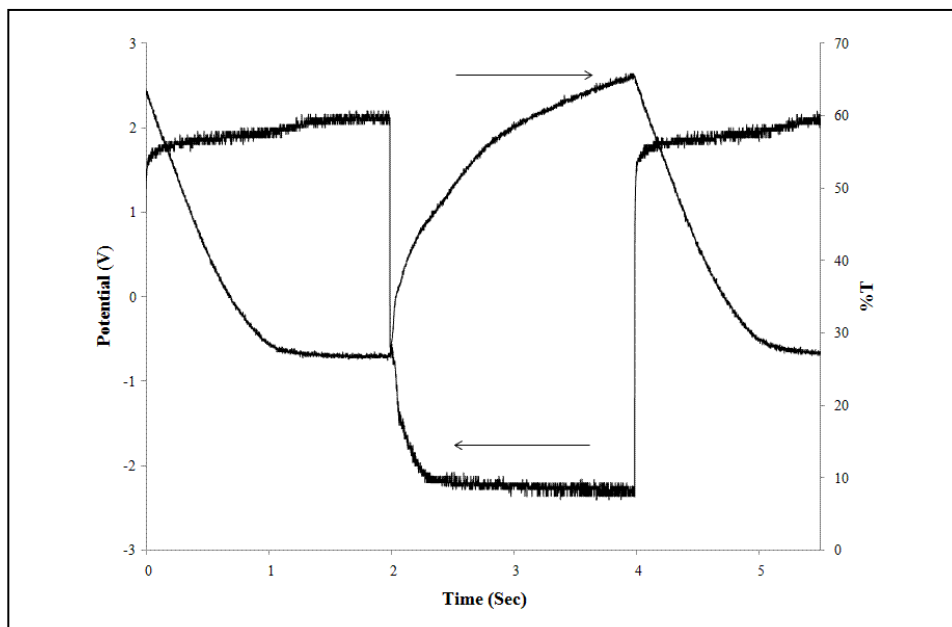


Figure 4-10. Switching speed response of (PANI/PASA)₄₀ asymmetric EC device during application of +/- 2.3 V square wave at 0.25 Hz.

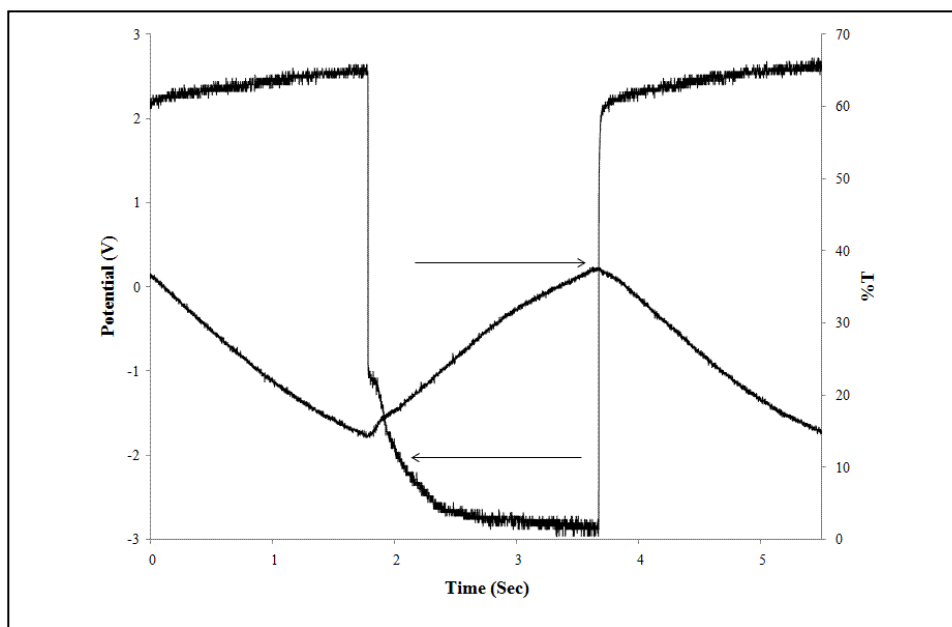


Figure 4-11. Switching speed response of (PANI/PAMPS)₄₀ asymmetric EC device during application of +/- 2.3 V square wave at 0.25 Hz.

4.4.5 Lifespan

PANI/PAMPS LbL films have been reported to degrade under application of ± 2.0 V potential.²³ In our study on PANI/PASA composites, the films showed reasonably long lifespan with little drop in performance. As shown in Figure 4-12, the contrast dropped by approximately 10% after undergoing more than one thousand cycles at an arbitrary sequence of $f = 1$ Hz and 0.25 Hz frequencies. The addition of PASA appears to have improved the lifespan of the system, yet more in depth study is needed to confirm this hypothesis.

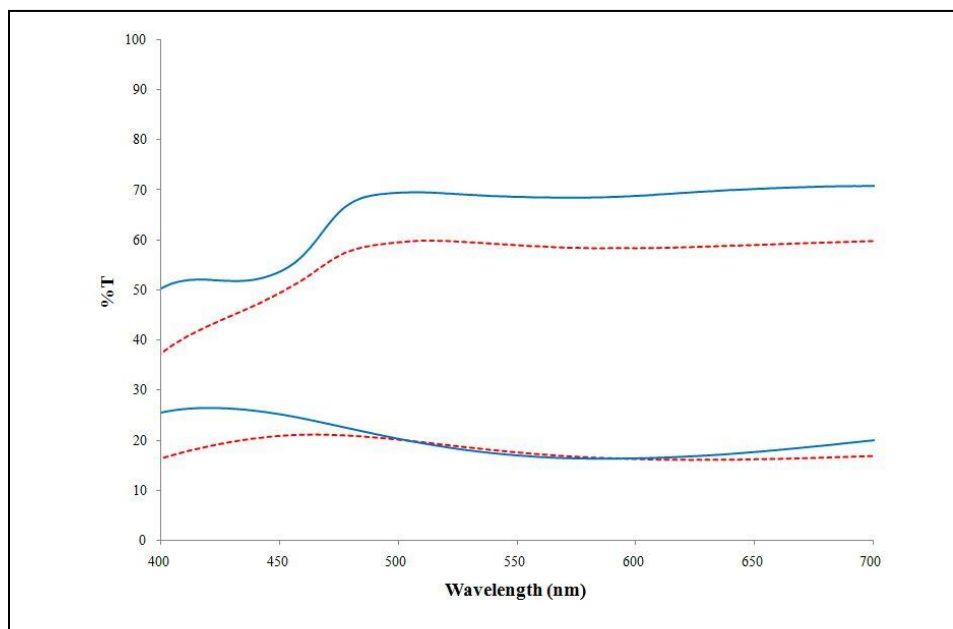


Figure 4-12. Spectra of $(\text{PANI/PASA})_{40}$ taken at -2.3 V and $+ 2.3$ V, before (solid line) and after (dotted line) going through more than 1000 switching cycles.

4.5 Conclusion

Dual electrochromic solid state electrochromic devices based on PANI and PASA were constructed based on LbL self-assembly. The devices exhibited high optical contrast over a wide range of wavelengths covering the entire visible spectrum. The average contrast of the 40-bilayer device in the visible spectrum was 49.7%. CV studies of the composite confirmed that both electrochromic polymers contribute to the electrochromic and electrochemical properties of the system, however PANI is primarily responsible for the observed transmittance changes. Comparison of PANI/PAMPS devices with PANI/PASA devices showed that the incorporation

of PASA to the composite increases the switching speed and lifespan of the device. The response time performance of the device was significantly improved by addition of PASA. Under application of +/- 2.0 V square wave at 0.25 Hz, the PANI/PASA device reached more than double the contrast compared to the PANI/PAMPS device. Thus, the addition of the conducting and electrochromically active PASA significantly improved the electrochromic and electrochemical properties of the composite.

4.6 References

1. Dauteront-Smith, W. C., *Displays* **1982**, 3, 3-22.
2. Mortimer, R. J., Electrochromic Materials *Chemical Society Reviews* **1997**, 26, 147-156.
3. Granqvist, C. G., Electrochromic tungsten oxide films: review of progress 1993-1998. *Solar Energy Materials and Solar Cells* **2001**, 60, 201-262.
4. Yano, J.; Higuchi, Y., Electrochromic properties of the polymer films derived from aniline derivatives and their dual-layer films. *Kobunshi Ronbunshu* **1990**, 47, (10), 817-824.
5. DeLongchamp, D. M.; Hammond, P. T., Multiple-color electrochromism from layer-by-layer-assembled polyaniline/Prussian blue nanocomposite thin films. *Chemistry of Materials* **2004**, 16, (23), 4799-4805.
6. Sonmez, G.; Meng, H.; Wudl, F., Organic Polymeric Electrochromic Devices: Polychromism with Very High Coloration Efficiency. *Chemistry of Materials* **2004**, 16, (4), 574-580.
7. Kim, E.; Jung, S., Layer-by-layer assembled electrochromic films for all-solid-state electrochromic devices. *Chemistry of Materials* **2005**, 17, (25), 6381-6387.
8. Choi, K.; Yoo, S. J.; Sung, Y. E.; Zentel, R., High contrast ratio and rapid switching organic polymeric electrochromic thin films based on triarylamine derivatives from layer-by-layer assembly. *Chemistry of Materials* **2006**, 18, (25), 5823-5825.
9. Jain, V.; Yochum, H.; Montazami, R.; Heflin, J., Millisecond switching in solid state electrochromic polymer devices fabricated from ionic self-assembled multilayers. *Applied Physics Letters* **2008**, 92, (3), -.
10. Jain, V.; Yochum, H.; Wang, H.; Montazami, R.; Hurtado, M.; Mendoza-Galvan, A.; Gibson, H.; Heflin, J., Solid-state electrochromic devices via ionic self-assembled multilayers (ISAM) of a polyviologen. *Macromolecular Chemistry and Physics* **2008**, 209, (2), 150-157.
11. G.A. Croker, B. G., N.J. Clecak, *Journal of Electro chemistry* **1979**, 126, 1339.
12. Riou, M. T.; Clarisse, C., THE RARE-EARTH SUBSTITUTION EFFECT ON THE ELECTROCHEMISTRY OF DIPHTHALOCYANINE FILMS IN CONTACT WITH AN ACIDIC AQUEOUS-MEDIUM. *Journal of Electroanalytical Chemistry* **1988**, 249, (1-2), 181-190.
13. Kobayashi, T.; Fujita, K.; Muto, J., Characteristics of electrochromic magnesium phthalocyanine films for repeated oxidation-reduction cycling. *Journal of Materials Science Letters* **1996**, 15, (14), 1276-1278.
14. Decher, G., Fuzzy Nanoassemblies: Toward Layered Polymeric Multicomposites. *Science* **1997**, 277, (5330), 1232-1237.
15. Hammond, P. T., Form and Function in Multilayer Assembly: New Applications at the Nanoscale. *Advanced Materials* **2004**, 16, (15), 1271-1293.
16. Stepp, J.; Schlenoff, J. B., *Journal of Electrochemistry* **1997**, 144, (L155).
17. DeLongchamp, D. M.; Kastantin, M.; Hammond, P. T., High-contrast electrochromism from layer-by-layer polymer films. *Chemistry of Materials* **2003**, 15, (8), 1575-1586.
18. Lutkenhaus, J. L.; Hammond, P. T., Electrochemically enabled polyelectrolyte multilayer devices: from fuel cells to sensors. *Soft Matter* **2007**, 3, (7), 804-816.
19. Ram, M. K.; Maccioni, E.; Nicolini, C., The electrochromic response of polyaniline and its copolymeric systems. *Thin Solid Films* **1997**, 303, (1-2), 27-33.
20. Lacroix, J. C.; Kanazawa, K. K.; Diaz, A., Polyaniline: A Very Fast Electrochromic Material. *Journal of the Electrochemical Society* **1989**, 136, (5), 1308-1313.
21. Bernard, M.-C.; Hugot-Le Goff, A.; Zeng, W., Elaboration and study of a PANI/PAMPS/WO₃ all solid-state electrochromic device. *Electrochimica Acta* **1998**, 44, (5), 781-796.
22. Hu, H. L.; Hechavarria, L.; Campos, J., Optical and electrical responses of polymeric electrochromic devices: effect of polyacid incorporation in polyaniline film. *Solid State Ionics* **2003**, 161, (1-2), 165-172.

23. Hechavarría, L.; Hu, H.; Rincón, M. E., Polyaniline-poly(2-acrylamido-2-methyl-1-propanosulfonic acid) composite thin films: structure and properties. *Thin Solid Films* **2003**, 441, (1-2), 56-62.
24. D. DeLongchamp; P. T. Hammond, Layer-by-Layer Assembly of PEDOT/Polyaniline Electrochromic Devices. *Advanced Materials* **2001**, 13, (19), 1455-1459.
25. Sarkar, N.; Ram, M.; Sarkar, A.; Narizzano, R.; Paddeu, S.; Nicolini, C., Nanoassemblies of sulfonated polyaniline multilayers. *Nanotechnology* **2000**, 11, (1), 30-36.
26. Yue, J.; Wang, Z. H.; Cromack, K. R.; Epstein, A. J.; MacDiarmid, A. G., Effect of sulfonic acid group on polyaniline backbone. *Journal of the American Chemical Society* **1991**, 113, (7), 2665-2671.
27. Wang, Y. Z.; Joo, J.; Hsu, C. H.; Epstein, A. J., Charge transport of camphor sulfonic acid-doped polyaniline and poly(o-toluidine) fibers: role of processing. *Synthetic Metals* **1995**, 68, (3), 207-211.
28. Shimizu, S.; Saitoh, T.; Uzawa, M.; Yuasa, M.; Yano, K.; Maruyama, T.; Watanabe, K., Synthesis and applications of sulfonated polyaniline. *Synthetic Metals* **1997**, 85, (1-3), 1337-1338.
29. Cheung, J. H.; Stockton, W. B.; Rubner, M. F., Molecular-level processing of conjugated polymers .3. Layer-by-layer manipulation of polyaniline via electrostatic interactions. *Macromolecules* **1997**, 30, (9), 2712-2716.
30. Clark, S. L.; Montague, M.; Hammond, P. T., Selective deposition in multilayer assembly: SAMs as molecular templates. *Supramolecular Science* **1997**, 4, (1-2), 141-146.
31. Ruths, J.; Essler, F.; Decher, G.; Riegler, H., Polyelectrolytes I: Polyanion/Polycation Multilayers at the Air/Monolayer/Water Interface as Elements for Quantitative Polymer Adsorption Studies and Preparation of Hetero-superlattices on Solid Surfaces. *Langmuir* **2000**, 16, (23), 8871-8878.
32. McAloney, R. A.; Sinyor, M.; Dudnik, V.; Goh, M. C., Atomic Force Microscopy Studies of Salt Effects on Polyelectrolyte Multilayer Film Morphology. *Langmuir* **2001**, 17, (21), 6655-6663.

Chapter 5: Highly Conductive, Transparent CNT Based Electrode for ECDs

Modification of Single-Walled Carbon Nanotube Electrodes by Layer-by-Layer Assembly for Electrochromic Devices

Published in Journal of Applied Physics, 2008, 103

Authors: Jain, V.; Yochum, H.; Montazami, R.; Heflin, J.R.; Hu, L.; Gruner, G.

5.1 Abstract

We have studied the morphological properties and electrochromic (EC) performance of polythiophene multilayer films on single wall carbon nanotube (SWCNT) conductive electrodes. The morphology for different numbers of layer-by-layer (LbL) bilayer on the SWCNT electrode has been characterized with atomic force microscopy and scanning electron microscope, and it was found that the LbL multilayers significantly decrease the surface roughness of the nanoporous nanotube films. The controlled surface roughness of transparent nanotube electrodes could be beneficial for their device applications. We have also fabricated EC devices with LbL films of poly[2-(3-thienyl) ethoxy-4-butylsulfonate/poly(allylamine hydrochloride) on SWCNT electrodes, which not only have high EC contrast but also sustain higher applied voltage without showing any degradation for more than 20 000 cycles, which is not possible in the case of indium tin oxide electrodes. Cyclic voltammetry of the LbL films formed on SWCNT shows higher current at low potential, revealing the feasibility of SWCNT electrode as a good host for electrolyte ion insertion.

5.2 Introduction

Thin single wall carbon nanotube (SWCNT) networks with thickness in the range of 10–100 nm have high sheet conductance while maintaining high optical transparency.^{1,2,3} These transparent electrodes have been used in organic solar cells, photovoltaic devices, and light emitting diodes, which show comparable device performance with indium tin oxide (ITO), along with better mechanical properties.^{4,5,6} SWCNT films are porous and have high surface area, which can be either bane or boon for the device application. The larger surface area ensures the availability of a higher amount of reactive sites at the SWCNT surface, but due to the rough

nature of the film, charge injection and light intensity can both be nonuniform and can occasionally shorten the device lifetime.⁷ To overcome this problem, we adopted the approach of coating the SWCNT film with the layer-by-layer (LbL) assembly; this helps in reducing the surface roughness and integrating the SWCNT into thin-film optoelectronic devices without short-circuiting the electrodes.

To achieve this, conformable coating of another layer is critical. Other techniques such as spin coating, solution casting, or electropolymerization, where rapid deposition of the material occurs, do not result in smooth films on rough surfaces. The Langmuir–Blodgett technique is one possible choice for developing such morphology, but it is preferred for flatter surfaces; the thickness of its individual layers cannot be varied as it is determined by the length of the molecule, it cannot smooth the surface, and also the electroactivity decreases for thicker films.⁸ In contrast to this, LbL deposited films not only decrease the surface roughness for uniform charge injection but also forms a nanoporous morphology which offers low resistance to charge and mass transfer.

Electrochromic (EC) devices undergo reversible color change in a material by the application of external voltage.⁹ LbL is also an excellent processing tool in the development of EC devices, as it provides flexibility and precise control over designing EC films on a diverse array of substrates with high uniformity and thickness control, higher contrast by the combination of multiple EC materials, and an increase in ionic conductivity for faster switching speeds.¹⁰ LbL films coated on SWCNT electrodes could potentially lead to better overall EC performance as compared to LbL films on ITO electrodes because of enhanced ion insertion, voltage sustainability, and increased life cycles. Several different groups have deposited modified carbon nanotubes on various substrates for different applications by the ionic LbL approach.^{11,12,13,14} In the present work, we have used LbL assembly on separately deposited conducting, transparent SWCNT electrodes rather than incorporate SWCNTs into LbL films. Carrillo *et al.*¹⁵ have used the LbL technique to coat the SWCNT surface with gold nanoparticles and polyelectrolytes, but their approach is more tedious and requires several steps of cross-linking. In addition, they deposited SWCNT through the chemical vapor deposition process, requiring catalysts for nanotube growth, which results in a nonuniform, low conductivity surface; hence, LbL deposition is random and unsuitable for electronic applications. In contrast, we have used a very well established technique of depositing uniform, highly conductive SWCNT films on large areas

through spray coating¹⁶ and combined the benefits of that method with a bottom-up LbL approach for highly stable EC devices.

5.3 Materials and Methods

SWCNT films on the glass have been deposited by spray coating with a similar procedure as explained in one of our previous work.¹⁶ Briefly arc-discharged single wall nanotube (Carbon Solutions Inc.) are dispersed in water with 0.5% sodium dodecyl sulfate with surfactants of 1 mg/ml. The solutions were sprayed onto glass or plastic substrates which were then heated to 80 °C. The water-soluble sodium polythiophene poly[2-(3-thienyl) ethoxy-4-butylsulfonate] (PTEBS) (Ref. 17) (American Dye Source) was used as the active EC material and bilayers were fabricated by the LbL deposition technique. EC PTEBS LbL devices have been characterized recently and good green to orange-red color changing properties have been obtained.¹⁸ Glass slides with a thin film of single-walled nanotubes were used as the substrate in the present work. The LbL deposition was performed by alternately dipping the SWCNT electrode in a positively charged aqueous polymeric solution, poly(allylamine hydrochloride) (PAH) (Sigma-Aldrich, $M_w \sim 75\ 000$, 10 mM concentration, pH 4), and negatively charged polymeric solution, PTEBS (1 mM, pH 4), for 6 min and rinsing in de-ionized water for 2 min.

5.4 Results and Discussions

Morphological studies of different numbers of PAH/PTEBS bilayers on SWCNT electrode by field emission scanning electron microscope (FESEM-LEO 1550) (Figure 5-1) at 5 kV and atomic force microscope (AFM) (Nanoscope IVa) (Figure 5-2) reveals that the LbL films are conformably coated onto the surface of the nanotube substrate. The AFM imaging was done in tapping mode with a cantilever of 50 N/m force constant and image size of $2 \times 2\ \mu\text{m}^2$ and 0–60 nm z scale. Due to the three-dimensional nanomesh network topology, the bare SWCNT electrodes with varied thickness of nanocomposite multilayers with pores show intriguing morphological properties. AFM scans of several LBL films confirmed that the films start wrapping around the nanotubes for the first few bilayers (two) and become a thick cylindrical film sheet around the nanotubes for a slightly higher number of bilayers (five); repeated scans were done at different locations to ensure that the morphological properties are similar throughout the sample. As can be clearly seen, the structure of the surface changes after deposition of a few bilayers and the film surface morphology smoothens as compared to the bare

SWCNT electrode. As material is deposited in each bilayer, moving from five to a higher number of bilayers (eight), the thin cylindrical sheets joined together to yield a nanoporous morphology. Sometimes, but not always, a few holes in the LbL film with more than eight bilayers were found. Continuation of the deposition to ten bilayers keeps the porosity in the film architecture but also increases the smoothness in the film. The plot of the surface roughness versus number of bilayers shows that the overall average surface roughness [R_a (nm)] of the deposited film decreases as the film thickness increases for higher numbers of bilayers; the bare SWCNT electrode has the highest surface roughness, which becomes nearly constant for films with ten or more bilayers. The decrease in surface roughness is caused by the subsequent multilayer deposition, which fills the voids in the SWCNT electrode and makes the surface smoother.

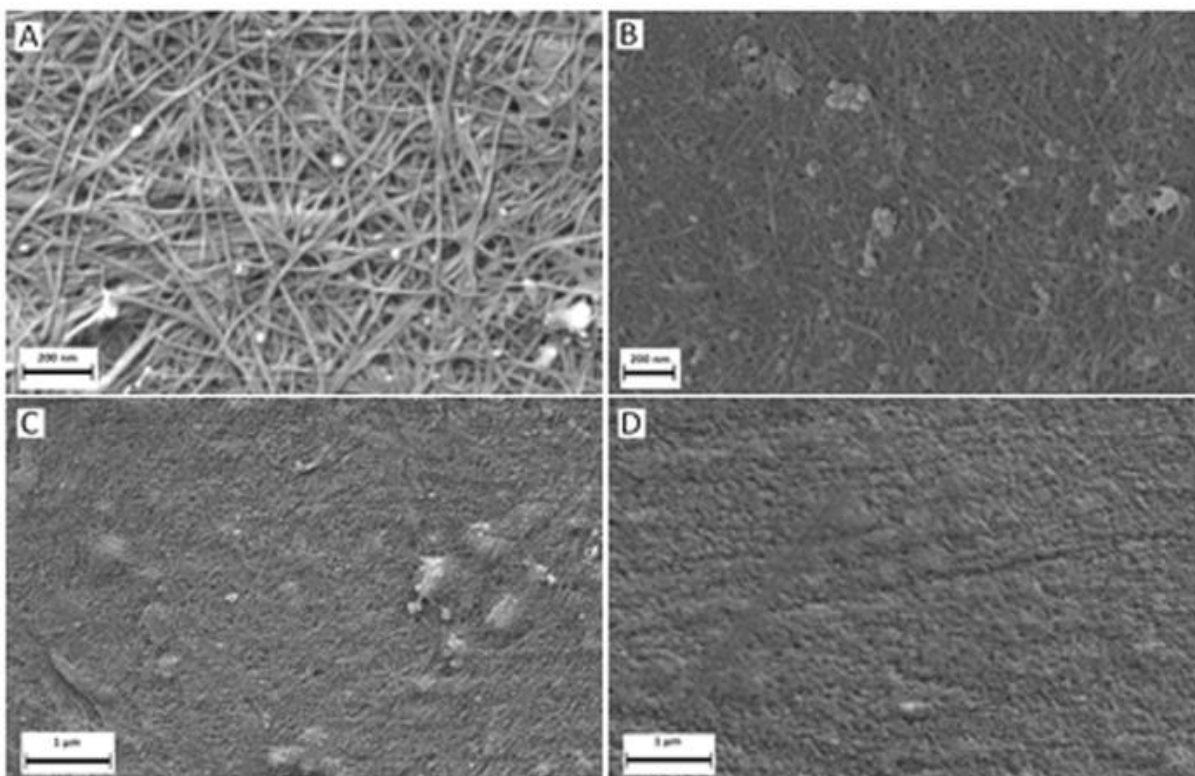


Figure 5-1. Scanning electron microscopy images of CNT electrode with (a) no film, (b) two bilayers, (c) five bilayers, and (d) ten bilayers of PAH/PTEBS film.

To study the redox activity of PAH/PTEBS multilayers on the SWCNT film, cyclic voltammetry (CV) experiments were performed with a computer-controlled potentiostat/galvanostat (PINE AFCBP1 bipotentiostat); all measurements were carried out in

LiClO₄ (0.1M)/acetonitrile with platinum (Pt) and AgCl/Ag as counterelectrode and reference electrode, respectively. The bare CNT electrode shows no electroactivity (Figure 5-3(a)) while the PAH/PTEBS LbL films clearly have a redox peak at around +0.10 V. The oxidation peak for the spin coated PTEBS film at the same conditions is at +0.6 V, but here the peak has shifted to a lower potential which reduces the impedance of the EC film and increases the electron transport efficiency.¹⁴ This is attributed to the highly porous nature of the SWCNT film. The peak did not skew to the lower peak voltage on increasing the scan rate, which suggests the negligible internal resistance of the LBL films and faster diffusion processes. The diffusion-controlled redox process was confirmed by a linear increase of current density peak with the square root of scan rate (Figure 5-3(b)) for a 40-bilayer film of PAH/PTEBS. It is important to note that the diffusion-controlled process provides maximum access to the film,¹⁹ which is attributed to complete ion intercalation and facile movement of ions in and out of the system and also brings long term stability (>20 000 cycles) to the device. The problems of ion porosity and diffusion have been observed with ITO electrodes as the low surface area brings more resistance for ionic movement and in some cases, the electrochemical reaction moves toward a surface controlled process rather than diffusion controlled.²⁰

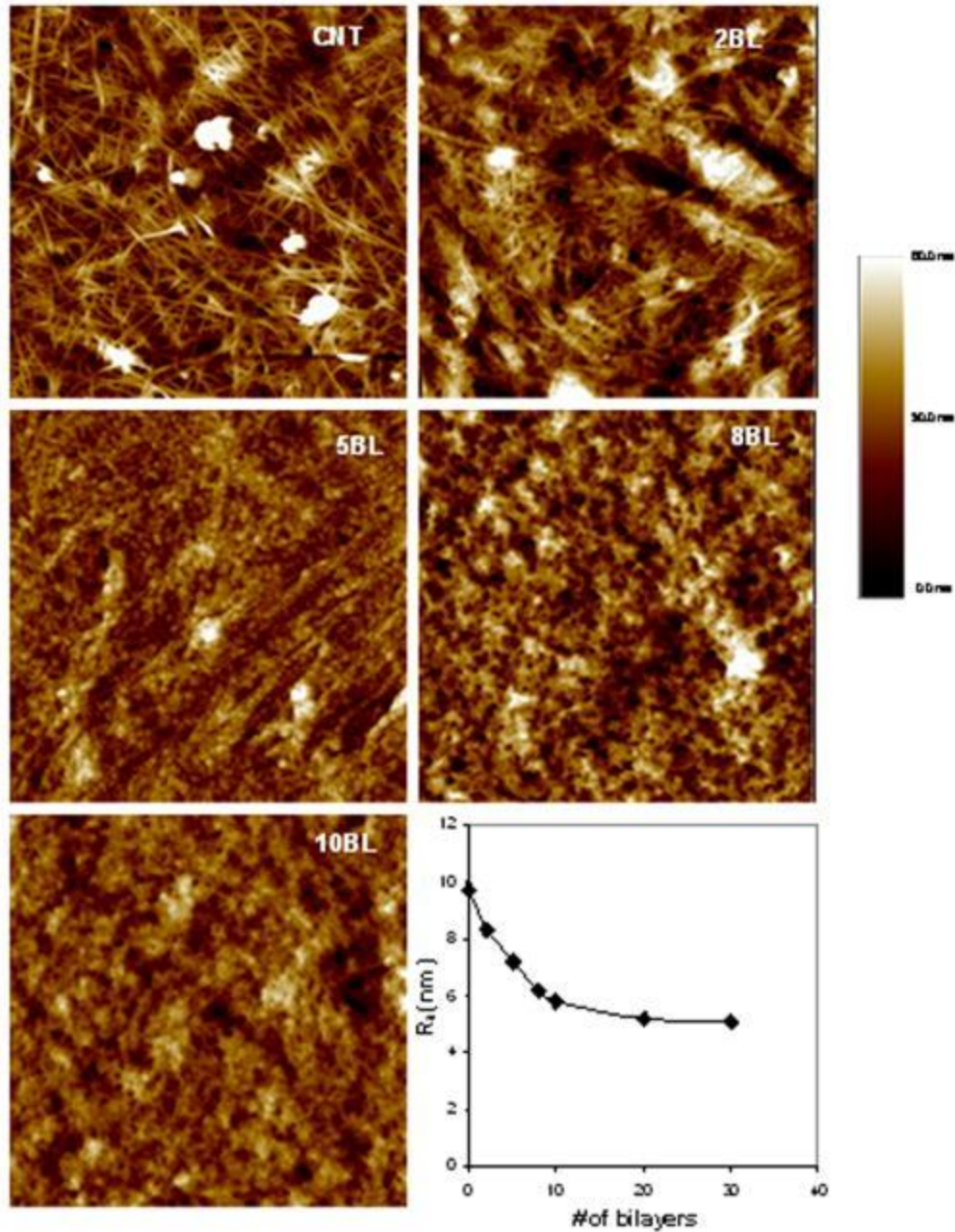


Figure 5-2. AFM height images of bare CNT electrode and film with two, five, eight, and ten bilayers. Area is $2 \times 2 \mu\text{m}^2$ and the z scale is from 0 to 60 nm. Also represented is the average surface roughness plot for different numbers of bilayers.

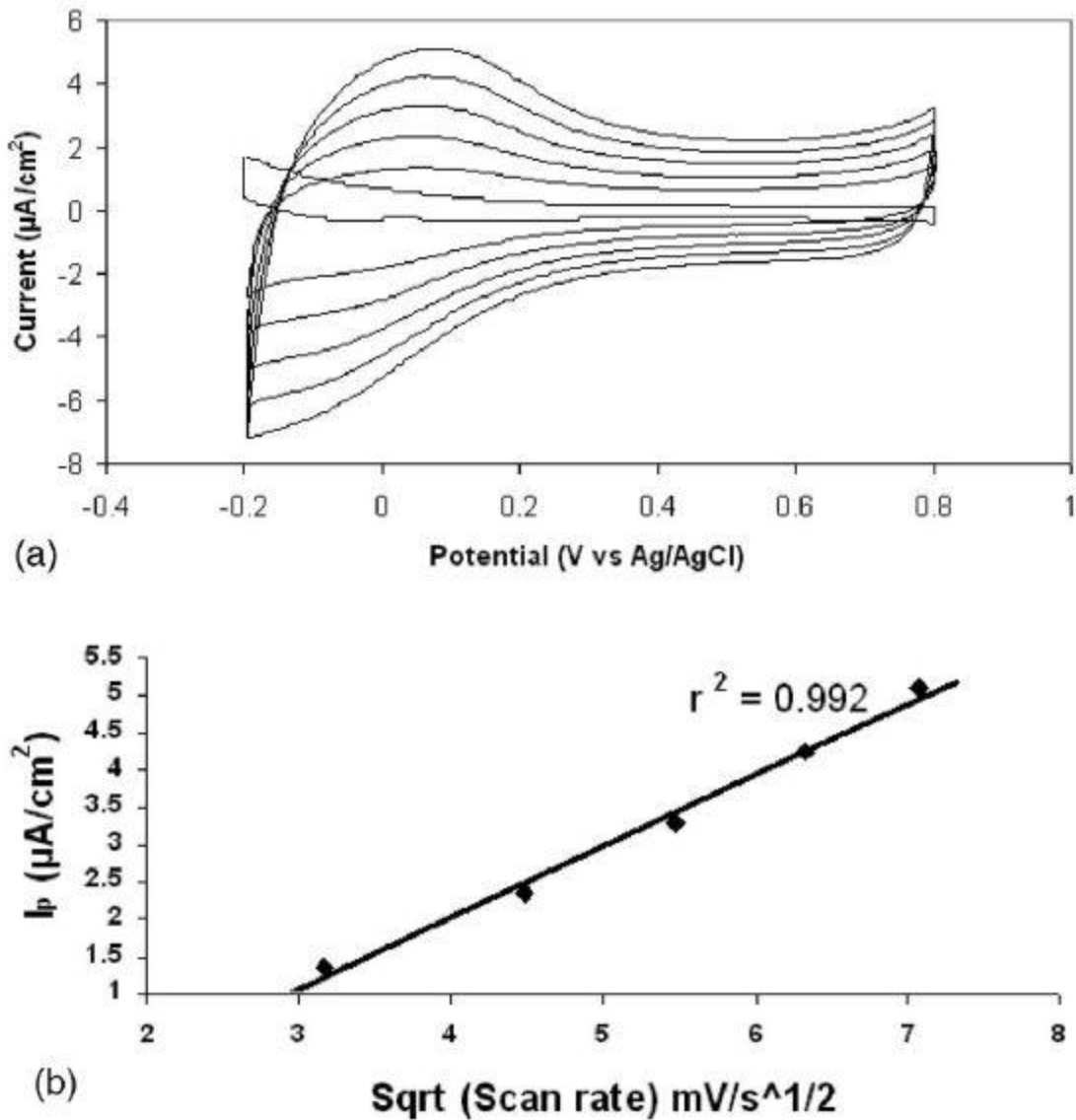


Figure 5-3. (a) CV of the bare CNT electrode at 10 mV/s and 40-bilayer film of PAH/PTEBS at 5, 10, 15, and 20 mV/s. (b) The linear relationship of peak current with the square root of scan rate.

The higher surface charge concentration of EC material on the SWCNT electrode is also confirmed by the large amount of charge intercalated in the system. The overall charge density (Q) calculated from CV experiment for PAH/PTEBS LbL film is $55 \mu\text{C}/\text{cm}^2$ for each bilayer deposited. The high PTEBS (PAH is electrochemically inactive) surface coverage for each

bilayer calculated by $\Gamma = Q/nF$ ($F=96.5 \times 10^3$ C/mol and $n=1$ is the number of electrons transferred) is 5.73×10^{-9} mol/cm², which is much higher ($\sim 10^{-10}$ – 10^{-11} mol/cm²) than the average surface coverage of polyelectrolytes for other LBL systems²¹ on ITO electrodes. The spectroelectrochemistry performance of EC devices on SWCNT electrodes has been evaluated by Perkin–Elmer Lambda 25 UV-visible spectrophotometer. Absorption spectra at different applied potentials (0.75–2.0 V) were measured with the EC LbL film on SWCNT electrode placed in a clear glass cuvette in 0.1M NaClO₄(aq) electrolyte solution. The base line was taken using a bare SWCNT electrode with no LbL film on it, which in itself has more than 80% transmission as compared to glass over a broad spectral range from visible to infrared. The *in situ* transmission spectrum (Figure 5-4) of a 40-bilayer PAH/PTEBS film on SWCNT film shows high EC contrast of 50% between the orange-red (bleached) state at 0 V and the dark green (colored) state at 2 V at λ_{max} of 735 nm. The EC device has no optical memory, and hence the film loses color as soon as the voltage supply is turned off. On stepwise increase in potential from 0.75 to 2.0 V, the absorption decreased at 410 nm due to the π - π^* transition of PTEBS and increased at the wavelength of 735 nm due to polaronic transitions. The contrast did not increase further for the application of >2.0 V, but the device was completely reversible for as high as 8–10 V of applied potential. This is in contrast to EC films on ITO, which suffer from the problem of not sustaining high voltages, leading to burning or degradation of the EC film. The EC coloration efficiency⁷ [$\Delta \text{OD} / \Delta Q$, where the optical density ΔOD is $\log(T_{\text{bleach}}/T_{\text{colored}})$ at a specific wavelength] calculated for the EC device (40 bilayers) was found to be 141 cm² C⁻¹ at 735 nm and is comparable to that obtained in related polythiophene materials.²²

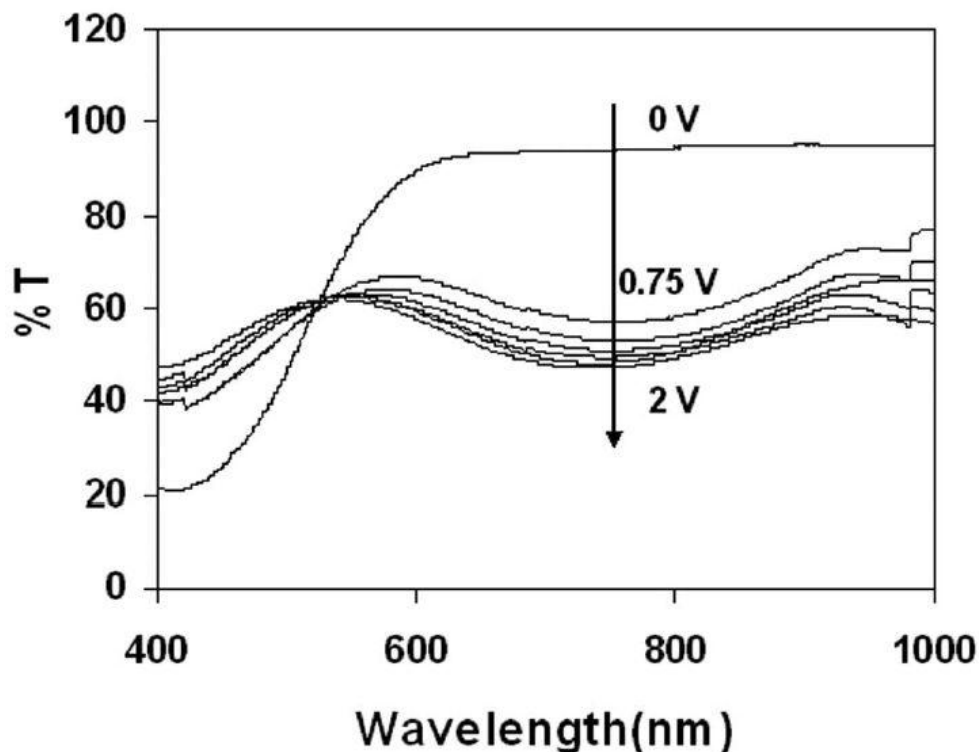


Figure 5-4. Change in transmission spectra of 40-bilayer PAH/PTEBS film on application of 0 V and step increase in voltage from 0.75 to 2.0 V

5.5 Conclusion

The LbL assembly on SWCNT film has been shown to effectively reduce the surface roughness as well as decrease the impedance and, based on CV measurements, increase the efficiency of ion transport. The improvement of the surface roughness by LbL modification may potentially improve the device performance of organic photovoltaic and organic light emitting diode devices with transparent SWCNT electrodes as anodes by improving the uniformity of charge injection. The high contrast (~50%) in our EC devices for long switching cycles and the ability to operate work at higher potential combined with a flexible substrate¹⁸ make it a good candidate for next generation e-paper displays as compared to flexible ITO substrates. The results show that the high surface coverage and charge of polyelectrolyte multilayers make the LbL-modified SWCNT film more tailored to specific application along with lower costs and environmentally friendly processing conditions. Future work will include a detailed study of EC and supercapacitor devices using such LBL-modified transparent SWCNT electrode.

5.6 References

1. Y. Zhou, L. Hu, and G. Grüner, *Appl. Phys. Lett.* **2006**, 88, 123109.
2. Z. Wu, Z. Chen, X. Du, J. M. Logan, J. Sippel, M. Nikolou, K. Kamaras, J. R. Reynolds, D. B. Tanner, A. F. Hebard, and A. G. Rinzler, *Science* **2004**, 305, 1273.
3. D. S. Hecht, L. Hu, and G. Grüner, *Appl. Phys. Lett.* **2006**, 89, 133112.
4. M. W. Rowell, M. A. Topinka, M. D. McGehee, H. Prall, G. Dennler, N. S. Sariciftci, L. Hu, G. Grüner, *Appl. Phys. Lett.* **2006**, 88, 233506.
5. D. Zhang, K. Ryu, X. Liu, E. Polikarpov, J. Ly, M. E. Tompson, and C. Zhou, *Nano Lett.* **2006**, 6, 1880.
6. J. Li, L. Hu, L. Wang, Y. Zhou, G. Grüner, and T. J. Marks, *Nano Lett.* **2006**, 6, 2472.
7. R. A. Hatton, N. P. Blanchard, A. J. Miller, and S. R. P. Silva, *Physica E* **2007**, 37, 124.
8. G. Decher, *Science* **1997**, 227, 1232.
9. P. M. S. Monk, R. J. Mortimer, and D. R. Rosseinsky, *Electrochromism: Fundamentals and Applications* **1995**, (VCH, Weinheim).
10. G. Decher and J. D. Hong, *Makromol. Chem., Macromol. Symp.* **1991**, 95, 321.
11. H. Paloniemi, M. Lukkarinen, T. Aarito, S. Areva, J. Leiro, M. Heinonen, K. Haapaka, and J. Lukkari, *Langmuir* **2006**, 22, 74.
12. K. J. Loh, J. Kim, J. P. Lynch, N. Wong, S. Kam, and N. A. Kotov, *Smart Mater. Struct.* **2007**, 16, 429.
13. J. H. Rouse and P. T. Lillehei, *Nano Lett.* **2003**, 3, 59.
14. M. Zhang, L. Su, and L. Mao, *Carbon* **2006**, 44, 276.
15. A. Carrillo, J. A. Swartz, J. M. Gamba, R. S. Kane, N. Chakarpani, B. Wei, and P. M. Ajayan, *Nano Lett.* **2003**, 3, 1437.
16. L. Hu, G. Gruner, J. Gong, C. Kim, and B. Hornbostel, *Appl. Phys. Lett.* **2007**, 90, 093124.
17. Q. Qiao, L. Su, J. Beck, and J. T. Mcleskey, Jr., *J. Appl. Phys.* **2005**, 98, 94906.
18. V. Jain, H. M. Yochum, R. Montazami, and J. R. Heflin, *J. Mater. Chem.* (unpublished).
19. D. DeLongchamp, M. Kastantin, and P. Hammond, *Chem. Mater.* **2003**, 15, 1575.
20. M. Gratzel, *J. Photochem. Photobiol.* **2003**, C 4, 145.
21. D. Ingersoll, P. J. Kulesza, and L. R. Faulkner, *J. Electrochem. Soc.* **1994**, 141, 140.
22. D. M. Welsh, A. Kumar, E. W. Meijer, and J. R. Reynolds, *Adv. Mater.* **1999**, (Weinheim, Ger.) 11, 1379.

Chapter 6: Conclusions and Recommendations

The ultimate goal of this research was to bridge between science foundations and engineering applications of electrochromic polymers and devices. Electrochromic devices have several applications including seven-segment displays, anti-glare mirrors and solar-attenuated windows and other possible future applications such as flat panel displays and optical switches. Construction of ECDs with higher transmittance contrast and faster switching speed is only possible through design or discovery of new materials or combinations of known materials combined with an optimum fabrication process. Control over the morphology of the thin films is just as important as the composition of the thin films, and it can be achieved via good understanding and control of the fabrication process and conditions.

In this thesis is presented design, fabrication, improvement, and study of ECDs based on electrochromic polymers. This thesis includes details about the quality and properties of the thin films based on several electrochromic polymers and two different designs, single and dual electrochrome ECDs. Also discussed in this thesis are the details of the fabrication technique and process, and effects of modulating the materials characteristics and assembly conditions.

Using different electrochromic polymers in different combinations led to several interesting results as well as general or detailed conclusions, which contribute to better understanding of the electrochromic materials and systems. ECDs with fast switching speed and high optical contrast were successfully designed and fabricated via the LbL assembly technique.

Modulating the assembly process conditions such as pH and ion concentration resulted in precise control over thickness and morphology of the electrochromic thin films. Control over these variables led to optimization of ECDs. Other ways to control the performance of the ECDs are through physical and electrical properties of the electrodes. Decreasing the active area of the electrode resulted in increase of the optical switching speed, and using electrodes with higher electric conductivity enhanced the performance of the device. A summary of the characteristics and properties of the ECDs discussed in this thesis is presented in Table 6-1; where t_c and t_d are coloration and decoloration times respectively.

A single electrochrome ECD was fabricated based on PEDOT:PSS as the electrochromic polymer. The device exhibited exceptionally fast switching speed on an active area of 60 mm^2 . A (PAH/PEDOT:PSS)₄₀ device exhibited optical switching speeds of 31 and 6 ms for coloration

and decoloration respectively. From the optical switching speed point of view, the coloration speed, $\sim 32\text{Hz}$, is the limiting factor yet still much faster ($>24\text{Hz}$) than the required frequency of video displays. Improvements on the contrast of PEDOT:PSS ECDs can possibly make this electrochromic system very desirable for construction of flat panel, low voltage video displays.

Generally, polyanilines have very good characteristics as electrochromic materials. However, the electrochromic properties of PASA, an electrochromic polymer from the polyaniline family, were not previously explored in much detail. Electrochromic properties of PASA thin films were studied in detail in this research. $(\text{PAH/PASA})_{40}$ electrochromic thin films were examined in electrochemical cuvette and exhibited good electrochromic properties under application of low voltage. PASA showed several redox states corresponding to color changes from dark blue to gray upon variation from oxidized to reduced states.

Integration of more than one electrochromic polymer in an electrochromic system brings interesting characteristics to the device. A dual electrochromic ECD was designed and fabricated based on PANI and PASA, both electrochromic polymers. $(\text{PANI/PASA})_{40}$ devices exhibited a large and flat change in transmittance over the visible spectrum, which is very rare and unique in ECDs. An ECD capable of transmitting/blocking the entire visible spectrum has several possible applications and is very attractive for green engineering and homeland security applications. This device also showed longer life span and faster optical switching speed compare to single electrochromic ECDs.

In addition to electrochromic materials and fabrication techniques, the characteristics of the electrode also contribute to the performance of the ECDs significantly. Electrodes with higher conductivity, transparency, and mechanical flexibility are highly desirable. An electrode based on carbon nanotubes was fabricated and tested with PTEBS as the electrochromic polymer. The new electrode sustained a higher voltage and also showed higher current flow through the ECD. The PTEBS ECD did not degrade for up to 20000 cycles, which is not achievable with widely used ITO electrodes.

Material(s)	$\Delta\%T-\lambda$	t_c (sec)	t_d (sec)	Electrode	Significance
PEDOT:PSS	35% - 580nm	0.031	0.006	ITO	fast optical switching
PASA	30% - 690nm	N/A	N/A	ITO	color memory, color change at both oxidation and reduction
PANI/PASA	~49.7%-vis. spec.	~2	~2	ITO	dual electrochrome, high contrast over entire vis. spectrum, lifespan
PTEBS	~50%-wide range	N/A	N/A	SWCNT	electrode, high contrast, lifespan

Table 6-1. Summary of the characteristics and properties of the ECDs discussed in this thesis

Materials and devices of higher quality are always in demand as the standards of electronic devices are rising at an exponential rate. It is strongly recommended to further improve the quality and performance of ECDs, especially the lifespan of the devices. A good approach for improving the ECDs, is to define the final application before improving the device. Some applications such as security windows do not require a very fast switching speed and the quality of the device depends more on the transmittance contrast whereas the quality of optical switches are more dependent on the switching speed but not the transmittance contrast as signal amplifiers can fill that gap. Improvements can be achieved by designing or finding new materials and by optimizing the fabrication process and improving the quality of the electrodes.

Overall, the work presented in this thesis confirms the high potential of ECDs to be commercialized, especially in the areas of green engineering and sustainable designs. Also it has been confirmed that LbL assembly technique has a diverse range of variables, of which the modulation and manipulation results in optimization of ECDs. The LbL assembly technique is an advantageous method for fabrication of functional thin films.